Received: 22 July 2021 | Revised: 28 February 2022 | Accepted: 2 March 2022

DOI: 10.1002/ar.24912

SPECIAL ISSUE ARTICLE

The Anatomical Record | WILEY

The effects of skull flattening on suchian jaw muscle evolution

Kaleb C. Sellers[1,2] | **Mauro Nicolas Nieto**[3] | **Federico J. Degrange**[3] | **Diego Pol**[4] | **James M. Clark**[5] | **Kevin M. Middleton**[1] | **Casey M. Holliday**[1]

[1]Department of Pathology and Anatomical Sciences, University of Missouri, Columbia, Missouri, USA

[2]Department of Clinical Anatomy and Osteopathic Principles and Practice, Rocky Vista University, Parker, Colorado, USA

[3]Centro de Investigaciones en Ciencias de la Tierra (CICTERRA), UNC, CONICET, Córdoba, Argentina

[4]CONICET, Museo Paleontológico Egidio Feruglio, Trelew, Argentina

[5]Department of Biological Sciences, The George Washington University, Washington, District of Columbia, USA

Correspondence
Kaleb C. Sellers, Department of Pathology and Anatomical Sciences, University of Missouri, Columbia, MO 65211.
Email: kalebsellers@gmail.com

Funding information
National Science Foundation (NSF-EAR 1631684 and 1636753); Society of Vertebrate Paleontology Estes Memorial Grant; Agencia Nacional de Promoción Científica y Tecnológica; Consejo Nacional de Investigaciones Científicas y Técnicas

Abstract

Jaw muscles are key features of the vertebrate feeding apparatus. The jaw musculature is housed in the skull whose morphology reflects a compromise between multiple functions, including feeding, housing sensory structures, and defense, and the skull constrains jaw muscle geometry. Thus, jaw muscle anatomy may be suboptimally oriented for the production of bite force. Crocodylians are a group of vertebrates that generate the highest bite forces ever measured with a flat skull suited to their aquatic ambush predatory style. However, basal members of the crocodylian line (e.g., *Prestosuchus*) were terrestrial predators with plesiomorphically tall skulls, and thus the origin of modern crocodylians involved a substantial reorganization of the feeding apparatus and its jaw muscles. Here, we reconstruct jaw muscles across a phylogenetic range of crocodylians and fossil suchians to investigate the impact of skull flattening on muscle anatomy. We used imaging data to create 3D models of extant and fossil suchians that demonstrate the evolution of the crocodylian skull, using osteological correlates to reconstruct muscle attachment sites. We found that jaw muscle anatomy in early fossil suchians reflected the ancestral archosaur condition but experienced progressive shifts in the lineage leading to Metasuchia. In early fossil suchians, musculus adductor mandibulae posterior and musculus pterygoideus (mPT) were of comparable size, but by Metasuchia, the jaw musculature is dominated by mPT. As predicted, we found that taxa with flatter skulls have less efficient muscle orientations for the production of high bite force. This study highlights the diversity and evolution of jaw muscles in one of the great transformations in vertebrate evolution.

KEYWORDS

biomechanics, Crocodylia, jaw muscles, skull

1 | INTRODUCTION

Feeding is one of the fundamental tasks faced by organisms, and so the feeding apparatus is thought to be under selective pressure (Dumont et al., 2009; Lauder, 1995; Santana et al., 2010). The acquisition of jaws and their associated musculature marked the final step in the transition from passive filter feeding to active predation in vertebrates (Gans, 1989; Gans & Northcutt, 1983) and has been linked with the evolutionary success of gnathostomes (Brazeau et al., 2017). Thus, jaw muscles are a key feature of the feeding apparatus (Herrel et al., 2005; Holliday & Witmer, 2007)

and essential to understanding the biomechanical consequences of morphological evolution documented by the fossil record.

Jaw muscle anatomy is constrained by the bony anatomy of the adductor chamber (Holliday & Witmer, 2007; Schumacher, 1973) and by diverse functional demands including the generation of bite force while permitting sufficient mandibular mobility (Ősi, 2014; Tseng & Wang, 2010). These constraints generally prevent the feeding apparatus from having optimal efficiency in most scenarios (Granatosky & Ross, 2020). The most efficient muscular geometry for producing high bite force using the lowest amount of jaw muscle without creating tensile joint loads would direct all of muscle force collinearly through the bite point in a single vector (Greaves, 1978). In such a system, the moment arm of each muscle vector and the moment arm of bite force would be equal, mechanical advantage would be one, and no joint forces would be produced. Additionally, in unilateral bites, contralateral muscle force can only produce bite force by lever action, in which case the optimal muscle orientation would be dorsoventral (Granatosky & Ross, 2020). Although musculoskeletal systems in which muscle forces act farther from the jaw joint than the location where biting occurs (i.e., systems with a mechanical advantage greater than one) are possible, such systems necessarily place the jaw joints under tensile loading (Huber et al., 2008). Amniote cranial joints are generally thought to be best suited to resisting compression (Greaves, 1978). Additionally, the architecture of the amniote skull rarely permits muscles to be placed sufficiently rostrally for the jaw muscle vector to act farther from the jaw joint than the bite point; instead, muscles act between the joint axis and the bite point, and the mandible acts like a lever even on the working side (Hylander, 1975). When muscle forces are not collinear, the muscle resultant (i.e., the magnitude of the vector sum of each muscle force; F_r) is less than gross muscle force (i.e., the scalar sum of each muscle force; F_g; Figure 1), as some portion of each muscle force is "spent" canceling each other. These components of muscle force do not contribute to bite force and are therefore "wasted" muscle force (Figure 1). This effect causes the mediolateral component of both hemimandibular muscle resultants to cancel the other. In taxa with caudally flat skulls like crocodylians, the flattened adductor chamber may cause jaw muscles to take on inefficient mediolateral orientations (Iordansky, 1964; Figure 1).

The evolution of crocodylians and their fossil relatives (i.e., the crocodyliforms) represents one of the great structural transitions in vertebrate evolution (Figures 2 and 3; Langston, 1973). Compared to primitive suchian ancestors, modern crocodylians have flat, robust, rigid skulls

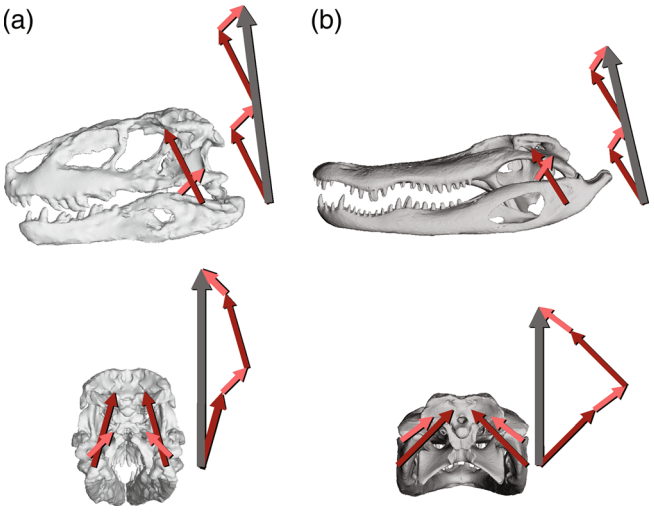

FIGURE 1 Non-collinear components of jaw muscles lower the effective applied force. (a) Prestosuchus and (b) alligator in left lateral view (top) and caudal view (bottom) with two hypothetical jaw muscles per side. Muscle 1 is dark red and 10 units long (representing 10 N) and Muscle 2 is pink and 5 units long (representing 5 N). (Note that different muscle orientations mean that a given vector will have different lengths in the two skulls in each view, but the total length is equal.) Each skull has an equal total length of force vectors, and so both skulls have equal total muscle force (i.e., Fg = 30 N). However, different orientations result in a larger muscle resultant in Prestosuchus (Fr ≈ 23.3 N) than in alligator (Fr ≈ 19.0 N), as a higher proportion of muscle force is used to counteract force of opposing orientation. A vector representation of the calculation of muscle resultant (individual muscles in dark red and pink, summing to the dark gray vector) lies to the right of each skull. Note that the orientation of the muscle vectors causes the resultant muscle force to be less than the total force exerted by the muscles (i.e., less than the total length of the red and pink vectors)

that are well-suited to resisting the high forces generated by feeding crocodylians. Crocodylians are thought to have relatively massive jaw muscles with novel attachments and deliver the highest measured static, crushing bite forces among vertebrates (Erickson et al., 2003), and powerful, whole-body thrashing and rolling augment these forces (Fish et al., 2007). The skull of crocodylians is strengthened by the sutural immobilization of plesiomorphically mobile joints and the acquisition of new intracranial and craniomandibular linkages (Clark et al., 2004; Langston, 1973; Pol et al., 2013). Thus, the evolutionary origin of crocodylians and their fossil relatives involved a substantial reorganization of the feeding apparatus.

The paucity of extant crocodylian species and relative ecological homogeneity belies the incredible diversity of feeding ecologies and accompanying craniodental anatomies found in extinct suchians (Brochu, 2001). Rather

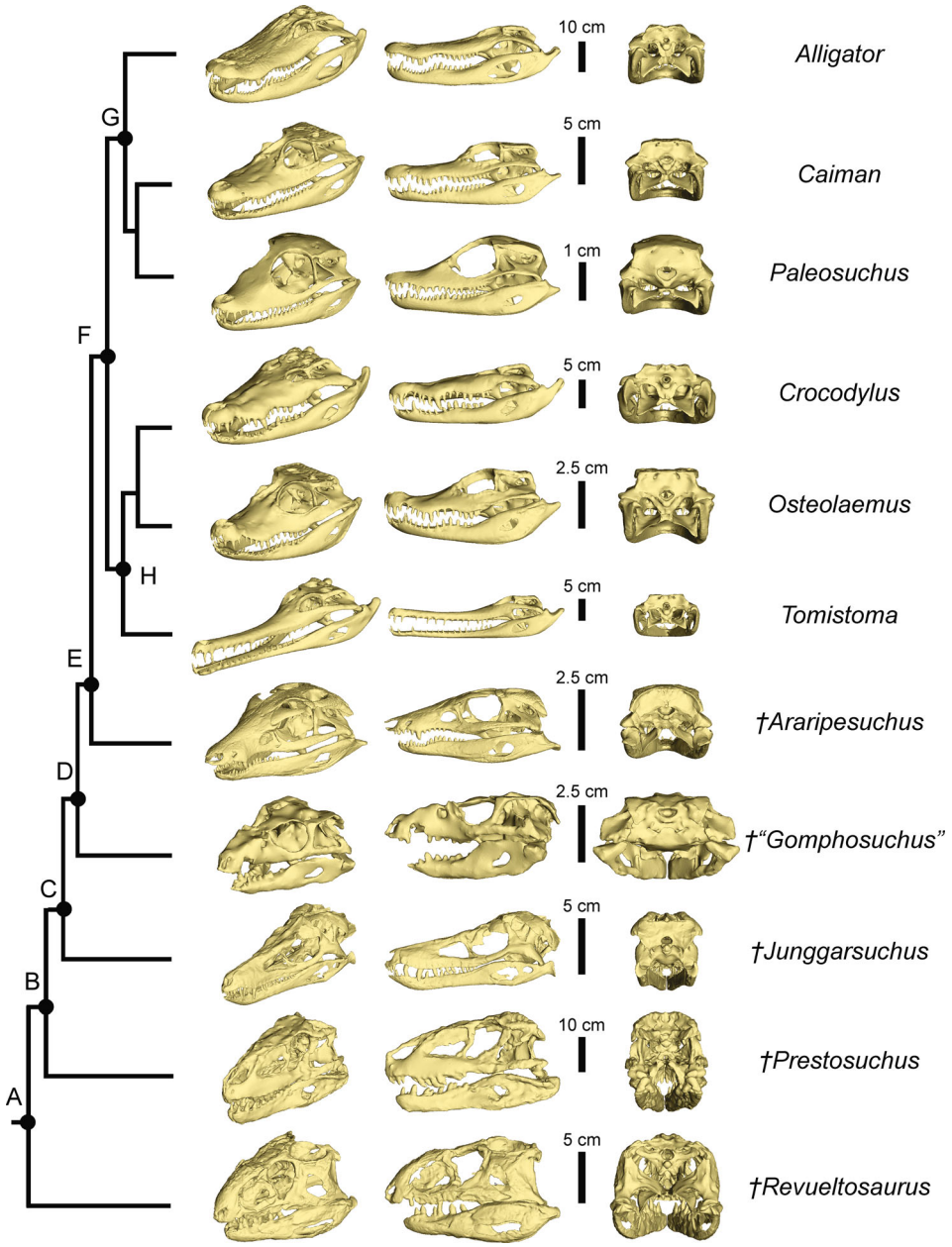

FIGURE 2 Suchian evolution was marked by progressive flattening of the skull. In this cladogram of our studied taxa, skulls are scaled to the same skull length. (a), Suchia; (b), Loricata; (c), Crocodylomorpha; (d), Crocodyliformes; (e), Metasuchia; (f), Crocodylia; (g), Alligatoridae; (h), Crocodylidae. Extinct taxa are indicated with dagger symbol (†)

than unmodified, primitive holdovers, the generalist crocodylians of today are just one tip of a tree full of terrestrial hypercarnivores, herbivores with oral processing, marine piscivore specialists, and taxa with bizarre morphologies adapted to uncertain feeding functions (Brochu, 2001; Cidade et al., 2019; Langston, 1973; Ősi, 2014; Wilberg, 2017). Extant crocodylians and many of their close fossil relatives have flattened skulls relative to basal suchians (Figure 2; Iordansky, 1973; Langston, 1973; Busbey, 1989, 1995). Although overall skull size is a primary predictor of muscle mass in various sauropsids (Gignac & Erickson, 2016; Herrel et al., 2005), the relative dimensions of the skull have been shown to impact muscle anatomy (Herrel et al., 2005) and bite force (Herrel et al., 2001) in avians and lepidosaurs. Thus, the lineage leading to Crocodylia has experienced substantial geometric changes to skull morphology including a flattened adductor chamber with more horizontally oriented muscles (Busbey, 1989; Schumacher, 1973).

Whereas most animals with relatively high bite forces show dorsoventrally tall skulls (Cost et al., 2019; Maynard-Smith & Savage, 1959; Menegaz et al., 2010;

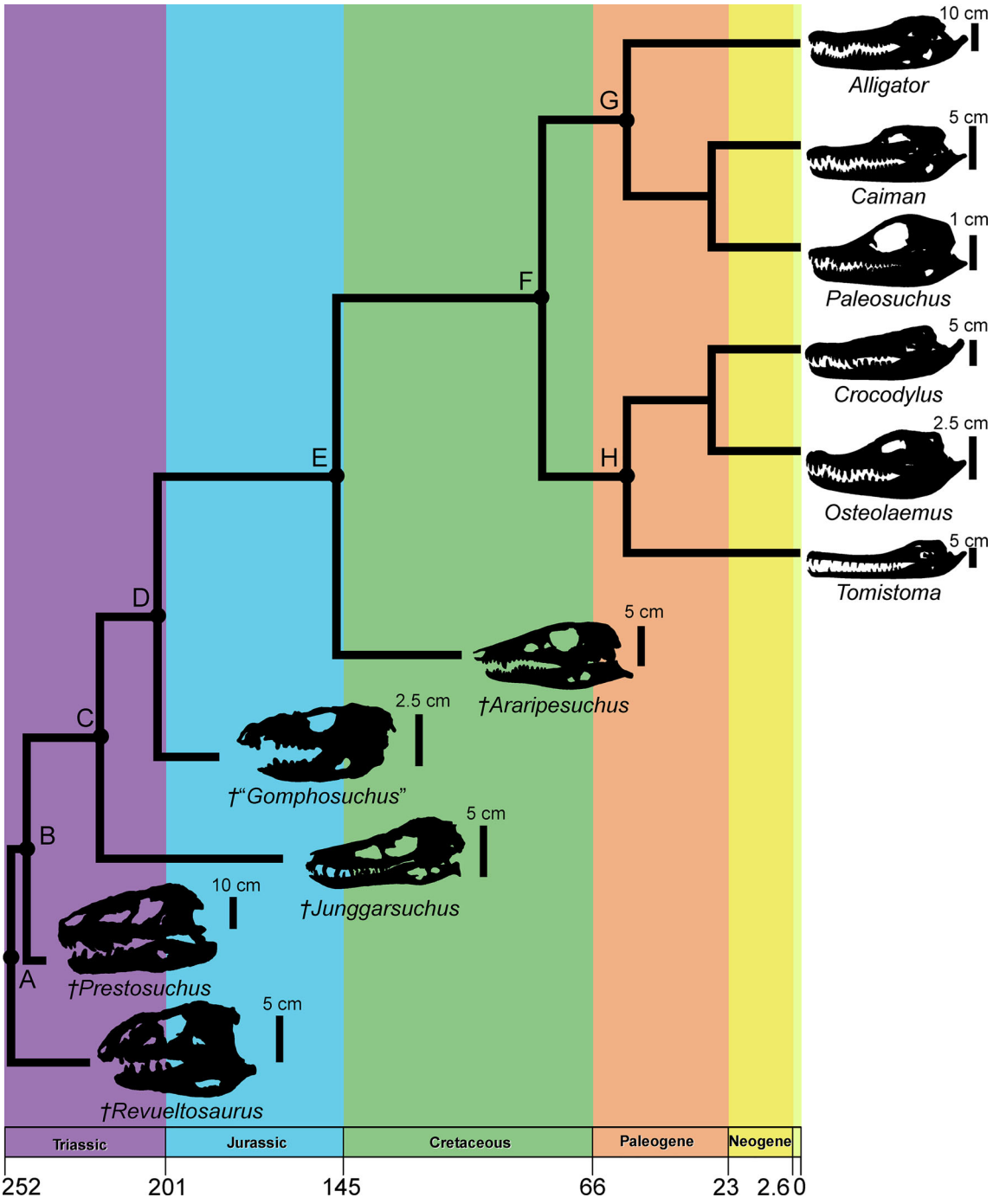

FIGURE 3 Time-calibrated phylogeny of sample. (a) Suchia; (b) Loricata; (c) Crocodylomorpha; (d) Crocodyliformes; (e) Metasuchia; (f) Crocodylia; (g) Alligatoridae; (h) Crocodylidae. Extinct taxa are indicated with dagger symbol (†)

Tseng & Stynder, 2011), extant crocodylians have characteristically flat skulls. A flat skull in a hard-biting animal therefore represents a biomechanical paradox: how to produce high feeding forces with biomechanically disadvantaged muscle orientations. The evolution of extant crocodylians and their fossil relatives, therefore, present an ideal opportunity to study the evolution of jaw muscle anatomy, skull shape, and biomechanical performance.

Here, we reconstruct jaw muscle anatomy across a phylogenetic range of crocodylians and fossil suchians to investigate the impact of skull flattening on jaw muscle anatomy. We use osteological correlates, the extant phylogenetic bracket (Witmer, 1995), dissections, and contrast-enhanced imaging to characterize jaw muscle anatomy in a sample of extant crocodylians and fossil suchians, quantify muscle efficiency, and determine how skull flatness influences jaw muscle geometry.

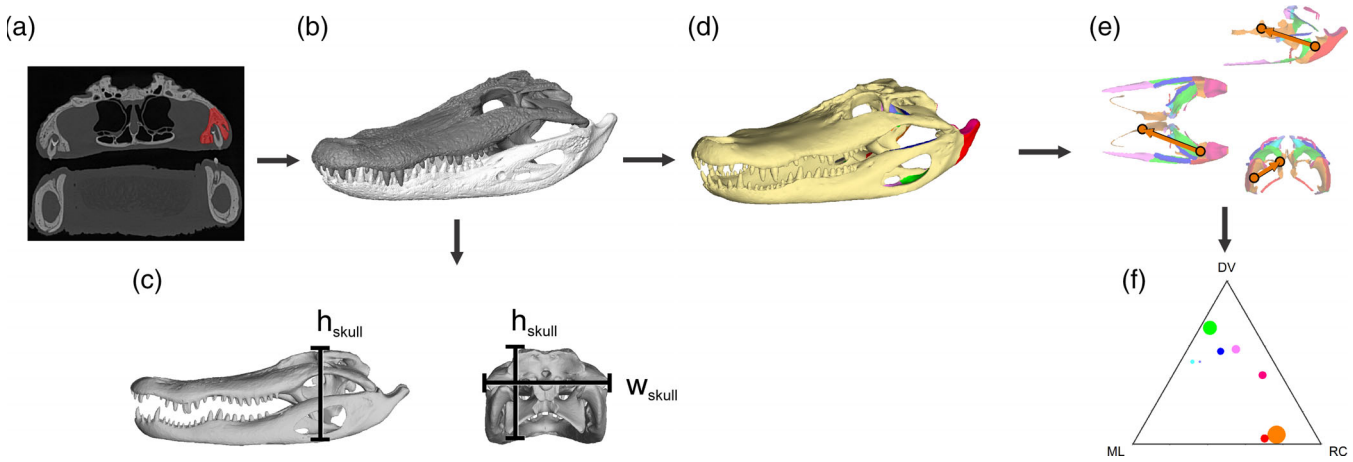

FIGURE 4 Methods used to estimate and quantify muscle force and geometry illustrated with *Alligator mississippiensis*. (a) CT or laser imaging data were acquired. (b) Digital 3D models of cranium and mandible were created. (c) Simple linear measures were acquired to characterize skull flatness. (d) 3D models were meshed into finite element models. (e) Muscle origins and insertions were mapped onto 3D models. (f) PCSA was calculated and used to estimate muscle force magnitude, and the centroids of muscle origins and insertions were used to calculate muscle force orientation. (g) Muscle force vector orientation was visualized using ternary diagrams

2 | AIMS AND PREDICTIONS

This study aims to characterize jaw muscle anatomy in a diverse sample of extant and extinct crocodylians and determine the effects of skull flattening on muscle performance in a lineage of species that evolved flat skulls yet still bite extremely hard. We use dissection, regular and contrast-enhanced tomography, and biomechanical modeling to reconstruct jaw muscle anatomy in digital models in a comparative sample of crocodylians and fossil relatives (Figures 2 and 3). We digitally mapped muscle attachment sites onto skulls and used them to estimate each jaw muscle's physiological cross-sectional area (PCSA) and thus its force (Figure 4). We used simple linear measurements to characterize skull size and flatness and explore the influence of skull shape and skull flatness on muscle force. We mapped these metrics of skull shape and biomechanical performance onto a phylogeny to reveal patterns of jaw muscle anatomical and functional evolution in crocodylians and their fossil relatives.

We hypothesize that skull flatness will negatively influence jaw muscle resultant force (Hypothesis 1) and that jaw muscles in taxa with flatter skulls will have more inefficient non-collinear orientations (Hypothesis 2). Crocodylians with flatter skulls may have traits to offset the impacts of inefficient jaw muscle orientation such as size-standardized larger gross muscle mass relative to extinct relatives (Hypothesis 3A). Alternatively, the muscle insertions may be placed relatively farther from the jaw joints, reflected in larger sums of size-standardized moment arms (Hypothesis 3B).

3 | MATERIALS AND METHODS

3.1 | Study specimens

The extant sample consisted of one individual from six extant crocodylian species (Table 1; Figures 2 and 3): *Alligator mississippiensis* (MUVC 008), *Caiman crocodilus* (FMNH 73711), *Paleosuchus palpebrosus* (FMNH 22817), *Crocodylus moreletii* (TMM M-4980), *Osteolaemus tetraspis* (FMNH 98936), and *Tomistoma schlegelii* (TMM M-6342). Data on extant crocodylian jaw muscles were collected by dissections and regular and contrast-enhanced computed tomography (CT) imaging. Additionally, key fossil suchians that represent important transitional stages were studied (Table 1; Figures 2 and 3): *Araripesuchus gomesii* (AMNH 24450), an undescribed "protosuchian" informally known as "*Gomphosuchus*" sp. (UCMP 97638; Clark, 1986), *Junggarsuchus sloani* (IVPP V14010), *Prestosuchus chiniquensis* (UFRGS PV0629T), and *Revueltosaurus callenderi* (PEFO 34561; Parker et al., 2021).

3.2 | Muscle modeling

To determine muscle force magnitudes and orientations, 3D models of specimens were created following Sellers et al. (2017). Specimens were scanned with CT or laser scanning. Three-dimensional bony anatomy was acquired by manually segmenting scan data with Avizo Lite 9.4 (FEI Visualization Science Group; https://www.thermofisher.com; Figure 4a,b). Using Geomagic Studio 2013 (Geomagic, Inc.; https://www.3dsystems.com), models were cleaned,

TABLE 1 Taxa included in this study

Taxon	Specimen number	Skull width (cm)	Skull height (cm)
Alligator mississippiensis	MUVC AL008	24.3	17.3
Caiman crocodilus	FMNH 73711	5.9	4.1
Paleosuchus palpebrosus	FMNH 22817	2.4	1.7
Crocodylus moreletii	TMM M-4980	16.8	8.9
Osteolaemus tetraspis	FMNH 98936	4.9	3.5
Tomistoma schlegelii	TMM M-6342	13.9	7.7
Araripesuchus gomesii[a]	AMNH 24450	4.8	3.4
"*Gomphosuchus*" *sp.*[a]	UCMP 97638	4.1	2.3
Junggarsuchus sloani[a]	IVPP V14010	5.5	5.2
Prestosuchus chiniquensis[a]	UFRGS PV0629T	23.5	21.6
Revueltosaurus callenderi[a]	PEFO 34561	9.3	7.1

[a]Extinct taxa.

smoothed, and aligned to global anatomical axes (i.e., x corresponds to mediolateral, y corresponds to dorsoventral, and z corresponds to rostrocaudal), and mandibles were opened to five degrees of gape. Models were meshed and filled with tetrahedra in Strand7 (Figure 4d). Muscular reconstructions in these taxa were informed by first-hand observations, regular and contrast-enhanced CT imaging, the literature (Busbey, 1989; Holliday & Witmer, 2007; Holliday & Witmer, 2009; Ősi, 2014), observations of closely related fossil taxa, and application of the extant phylogenetic bracket (Witmer, 1995). All muscle terminology follows Holliday and Witmer (2007). Physiological cross-sectional area (PCSA) is calculated by combining information about attachment site geometry and muscular parameters, described in Equation 1 (Sacks & Roy, 1982):

$$\mathrm{PCSA} = \frac{\mathrm{V_M}}{\mathrm{l_f}} \times \cos(\theta), \tag{1}$$

where V_M is the volume of the muscle, l_f is the fiber length of the muscle, and θ is the angle of pennation. We estimated muscle volume by modeling each muscle attachment site as one face of a frustum, defined as follows:

$$\mathrm{V_M} = \frac{\mathrm{l_M}}{3} \times \left(\mathrm{A_{or.}} + \mathrm{A_{ins.}} + \sqrt{\mathrm{A_{or.}} \times \mathrm{A_{ins.}}}\right), \tag{2}$$

where $A_{or.}$ is the area of the muscle origin and $A_{ins.}$ is the area of the muscle insertion.

The ratio between PCSA and force produced is specific tension, defined as

$$\mathrm{F_M} = \mathrm{PCSA} \times \mathrm{T_{specific}}, \tag{3}$$

where F_M is the muscle force and $T_{specific}$ is the specific tension. Muscular parameters that could not be estimated directly from fossil morphology (e.g., relative length of muscle fibers, specific tension, etc.) were given values from *Alligator* (sensu Porro et al., 2011). The effects of pennation on muscle force are minimal over the range of variation occupied by the vast majority of vertebrate muscles (Bates & Falkingham, 2018; Cost et al., 2019), and jaw muscle pennation in sauropsids is generally conservative (Cost et al., 2019; Wilken et al., 2019, 2020). Relative fascicle length has greater impact on muscle force (Bates & Falkingham, 2018) but is rarely reported in the literature. Thus, the use of *Alligator* muscle architecture is a conservative estimate justified for a broad comparative study; any biases introduced by using *Alligator* data would be toward no difference. To determine muscle orientation, the muscle vector was calculated by subtracting the centroid of the insertion from the centroid of the origin, shown as follows:

$$(x,y,z) = (x_{or.} - x_{ins.}, y_{or.} - y_{ins.}, z_{or.} - z_{ins.}), \tag{4}$$

where x, y, and z are, respectively, the mediolateral, dorsoventral, and rostrocaudal components of the muscle vector, $x_{or.}$, $y_{or.}$, and $z_{or.}$ are, respectively, the mediolateral, dorsoventral, and rostrocaudal coordinates of the centroid of the muscle origin, and $x_{ins.}$, $y_{ins.}$, and $z_{ins.}$ are, respectively, the mediolateral, dorsoventral, and rostrocaudal coordinates of the centroid of the muscle insertion (Figure 4e). Areas and centroids of muscle origins and insertions were obtained using a modified version of the Area_Centroids_From_STL script (Davis et al., 2010; Santana et al., 2010). To compare functional muscle anatomy across this sample, muscle vectors were

projected into ternary space and visualized using ggtern (Hamilton & Ferry, 2018; Cost et al., 2019; Wilken et al., 2020; Figure 4f).

3.3 | Skull flatness and muscle efficiency

Skull size and proportions are known to be primary determinants of muscle force. We measured two linear distances of the caudal skull used in recent functional and morphological studies of crocodylians (Iijima, 2017; O'Brien et al., 2019) that capture the size of the adductor chamber: the dorsoventral distance between the ventral margin of the pterygoid flange and the dorsal margin of the skull table (skull height; h_{skull}; Figure 4c; "pterygoid flange depth" of Iijima, 2017) and the maximum mediolateral width at the quadrate condyles (skull width; w_{skull}; Figure 3c; "head width" of O'Brien et al., 2019).

For producing useful bite force, noncollinear muscle vectors are less efficient than collinear vectors, because some component of noncollinear vectors is "lost" canceling out one another and does not contribute to bite force production. These components represent "wasted" muscle force (Figure 1). Systems with more collinear jaw muscles thus apply loads with less muscle tissue. The total amount of muscle force acting on the jaws has been reported in two ways: muscle resultants and total muscle force. Muscle resultants are calculated by taking the vector sum of every jaw muscle force vector acting in the skull (Clausen et al., 2008; Greaves, 1982; Greaves, 2000; Perry et al., 2011; Weijs et al., 1987). Total muscle forces are calculated by taking the scalar sum of the magnitude of every jaw muscle force vector acting in the skull (Cox et al., 2012; Porro et al., 2011; Sellers et al., 2017). To estimate the degree of wasted muscle force in each taxon, we calculated "muscle efficiency" as ratio of the magnitude of the muscle resultant and gross muscle force, as defined in Equation (3):

$$E_M = \frac{F_r}{F_g} = \frac{\| \vec{v}_{res} \|}{\sum \| \vec{v}_{musc_i} \|} = \frac{\| \sum \vec{v}_{musc_i} \|}{\sum \| \vec{v}_{musc_i} \|}, \quad (5)$$

where E_M is muscle efficiency, F_r is resultant muscle force, F_g is gross muscle force, $\vec{v}_{res}$ is the resultant of all muscle vectors, and $\vec{v}_{musc_i}$ is the muscle vector of the ith muscle. As muscle geometry becomes more collinear and as muscles lose mediolateral components, this ratio approaches unity (Figure 1).

3.4 | Statistical analyses

Although we hypothesize that the ratio of skull height and skull width is important for muscle force, these measures of size are highly correlated, and thus neither can be used to account for size. Thus, we performed a principal components analysis (PCA) on the two linear measurements after Z-standardization. PCA of skull width and skull height produced a variable linked with overall size (PC1; eigenvector: (−0.707, −0.707; eigenvalue: 1.95; 97.6% of variance explained; Figure 5a,b) and a variable that approximately corresponds with aspect ratio, or skull height over skull width (PC2; eigenvector: [−0.707. 0.707]; eigenvalue: 0.048; 2.4% of variance explained; Figure 5a,c). Both skull width and skull height load strongly negatively on PC1, suggesting PC1 is representative of skull size. Skull height loads positively on PC2, but skull width loads negatively. This suggests that PC2 represents the inverse relationship between these variables, and PC2 is highly correlated with skull height divided by skull width (correlation coefficient = .85; Figure 5c). Thus, PC2 will be used to represent the size-independent aspect ratio of the skull in caudal view (i.e., the inverse of skull flatness).

To test our hypothesis that skull flatness influences muscle force (Hypothesis 1), we used phylogenetic generalized least-squares (PGLS) regression of muscle force against PC1 and PC2 using a time-scaled phylogeny modified from Nesbitt (2011) and Wilberg et al. (2019). We modeled the muscle resultant force (F_r) against PC1, (Model 1.1), PC2 (Model 1.2), and PC1 + PC2 (Model 1.3), for a total of three models (Table 5). To determine the most appropriate models of muscle force, we calculated the Akaike Information Criterion for each model, corrected for small sample size (AICc). For each hypothesis, the model with the highest AICc weight was considered the best model. A best-fit model of F_r that includes PC2 would support Hypothesis 1.

To test our hypotheses of the relationship between skull shape and muscle geometry, (Hypothesis 2), we used PGLS regression of muscle efficiency (E_M) against PC1, (Model 2.1), PC2 (Model 2.2), and PC1 + PC2 (Model 2.3), for a total of three models (Table 5). A best-fit model of E_M that includes PC2 would support Hypothesis 2, whereas a nonexistent or negative relationship would fail to lend support.

To test our hypothesis that the effects of flat skulls on muscle biomechanics are "mitigated" by higher muscle mass, (Hypothesis 3A), we used PGLS regression of the gross muscle force (F_g) against PC1, (Model 3.1), PC2 (Model 3.2), and PC1 + PC2 (Model 3.3), for a total of three models (Table 5). A best-fit model for gross muscle force including a term for PC2 would support the hypothesis that these skulls rely on extra muscle mass. To test our hypothesis that inefficient muscle geometries are "mitigated" by longer moment arms of muscles (Hypothesis 3B), we used PGLS regression of the sum of muscle moment arms against PC1, (Model 3.4), PC2 (Model 3.5), and PC1 + PC2

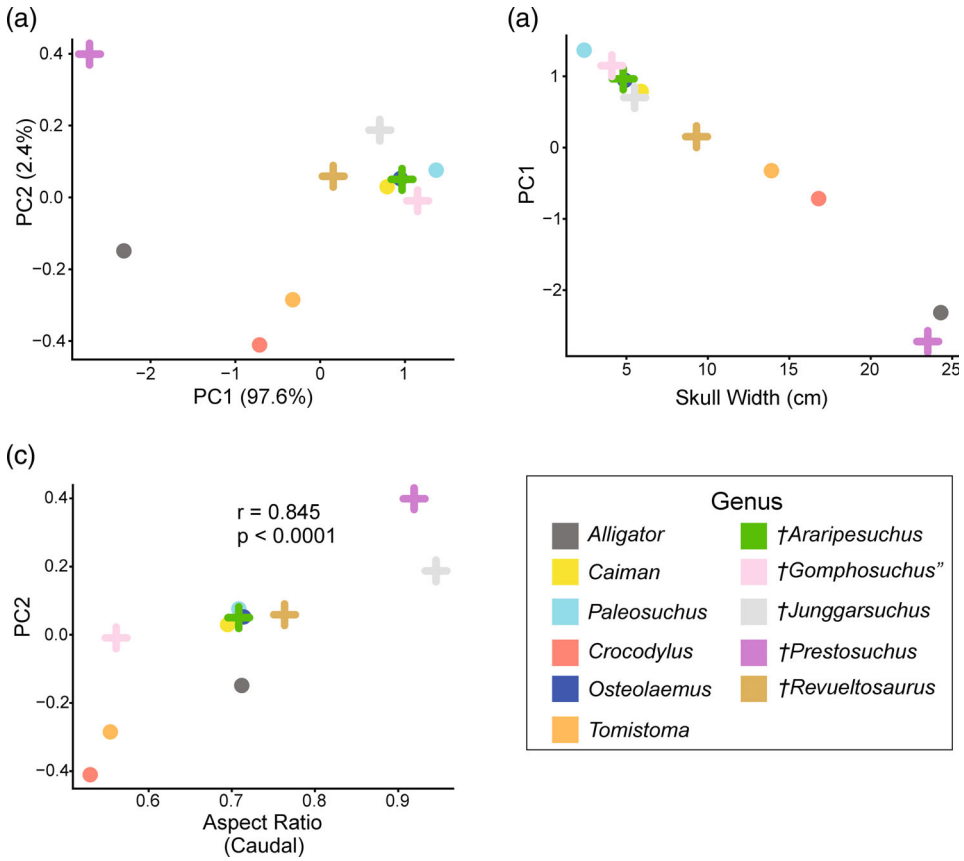

FIGURE 5 Results of principal components analysis of skull measurements. (a) PC1 versus PC2. Note that PC1 is related to negative size, so larger skulls are to the left of the plot. (b) PC1 vs skull width (a proxy for skull size). (c) PC2 versus aspect ratio of skulls in caudal view (i.e., hskull/wskull). In all plots, fossil taxa are represented by crosses whereas extant taxa are circles. Extinct taxa are indicated with dagger symbol (†)

(Model 3.6), for a total of three models (Table 5). A significant relationship between the moment arms and skull flatness supports the hypothesis that taxa with flat skulls use larger moment arms to mitigate inefficient muscular orientations. All statistical analyses were carried out using R (R Core Team, 2021).

4 | RESULTS

4.1 | Organization of results

First, we briefly summarize the primitive condition for suchian jaw muscle anatomy based on comparisons among extant archosaurs and the literature. Next, we describe major derived features of the extant crocodylian jaw musculature, then evaluate osteological correlates in select fossil suchians to assess the phylogenetic history of these character changes in the context of our 3D muscle-mapped models (Figures 6–10; Figures A1-A11). Finally, we present the results of our quantitative analyses and hypothesis testing.

4.2 | Primitive condition for suchian jaw muscles

Early suchians lack many of the osteological correlates of jaw muscles that are found in the skulls of extant crocodylian jaw muscles. In particular, the adductor tubercle of the quadrate for the tendinous attachments of musculus adductor mandibulae posterior (mAMP), the cotylar crest of the laterosphenoid for the attachment of m. pseudotemporalis superficialis (mPSTs), and the coronoid eminence of the surangular for the tendinous attachment of the temporal muscles tend to be less well developed in crocodylomorphs with plesiomorphic anatomy (Holliday & Witmer, 2009; Ősi, 2014). Thus, our reconstruction of early suchian jaw muscle anatomy is broadly comparable to those of typical sauropsids (Holliday & Witmer, 2007, 2009). The internal mandibular adductor (mAMI) is separated into the pseudotemporalis (mPST) and pterygoid (mPT) bellies. mPSTs originates on the medial border of the dorsotemporal fenestra and the lateral face of the laterosphenoid and inserts on the mandible rostral to the

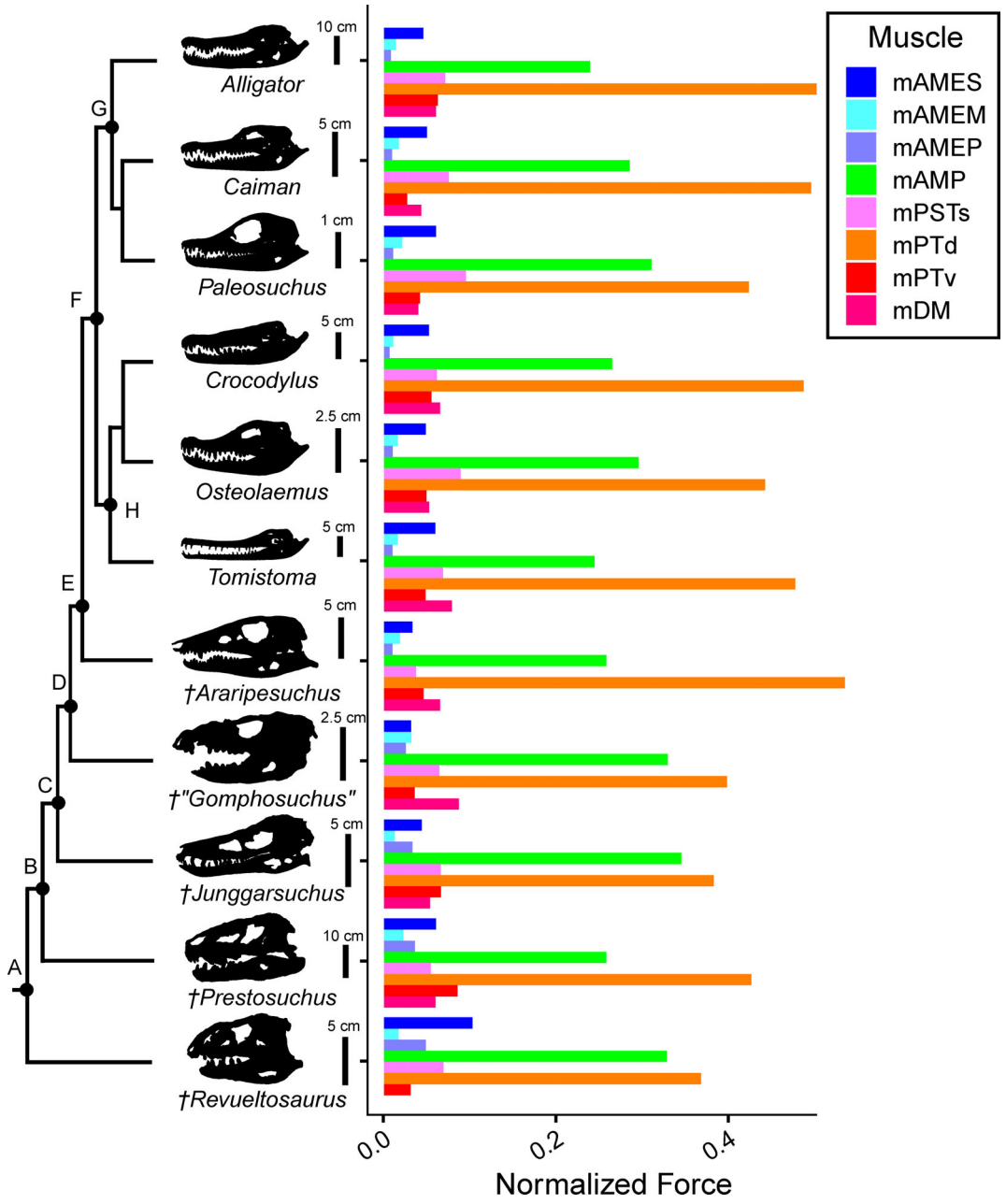

FIGURE 6 Muscle proportions subtly changed over suchian evolution. Musculus pterygoideus dorsalis (mPTd) and musculus adductor mandibulae posterior (mAMP) were of approximately equal size in early suchians, but in extant crocodylians, mPTd is approximately twice the size of mAMP and accounts for at least ~40% of total muscle force. (a) Suchia; (b) Loricata; (c) Crocodylomorpha; (d) Crocodyliformes; (e) Metasuchia; (f) Crocodylia; (g) Alligatoroidea; (h) Crocodyloidea. Extinct taxa are indicated with dagger symbol (†)

adductor fossa. Musculus pterygoideus dorsalis (mPTd) retains a primitive morphology in early suchians; its origin is on the lateral surface of the palatine and the lateral surface of the quadrate ramus and caudoventral aspect of the pterygoid flange of the pterygoid bones, and this muscle inserts only onto the medial surface of the articular bone. The external mandibular adductors (mAME) originate around the edges of the dorsotemporal fenestra and inserts onto the surangular shelf and coronoid bone. The primary jaw opener, depressor mandibulae (mDM), originates on the exoccipital and inserts onto a short retroarticular process. The mAMP originates on the body and pterygoid ramus of the quadrate and inserts onto the adductor fossa.

4.3 | Extant Crocodylian jaw muscles

In extant crocodylians, various muscles have altered bony attachments associated with structural changes in the skull.

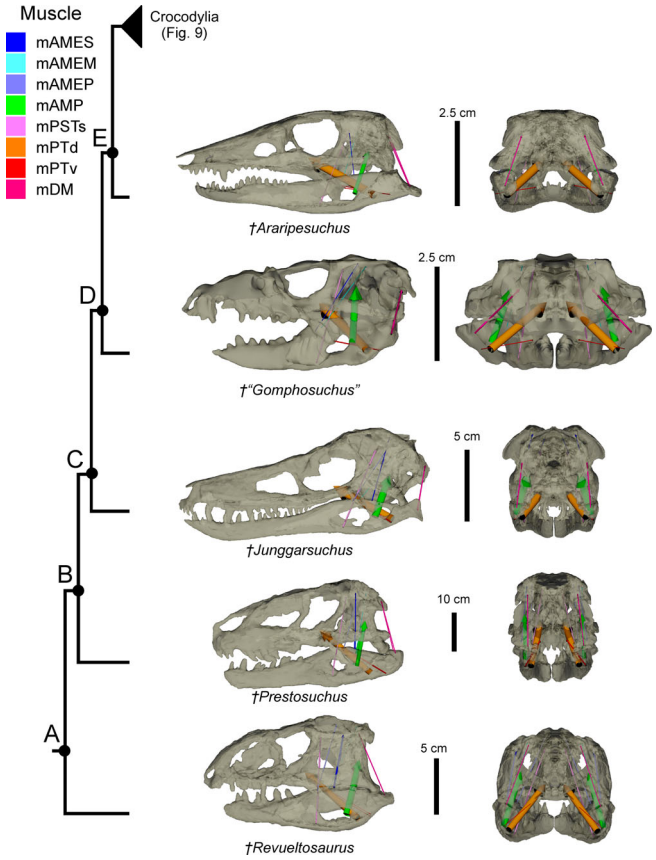

FIGURE 7 Suchian jaw muscle anatomy progressively shifted in the lineage leading to Crocodylia. Reconstructed muscle resultants and accompanying ternary diagrams are displayed for select taxa that characterize changes to muscle anatomy during suchian evolution. Vector thickness and size of the matching point on ternary diagrams correspond to normalized muscle force. Models are scaled to the same skull height. (a) Suchia; (b) Loricata; (c) Crocodylomorpha; (d) Crocodyliformes; (e) Metasuchia. Extinct taxa are indicated with dagger symbol (†), Table A1 contains links to Sketchfab models of skulls with reconstructed muscle vectors

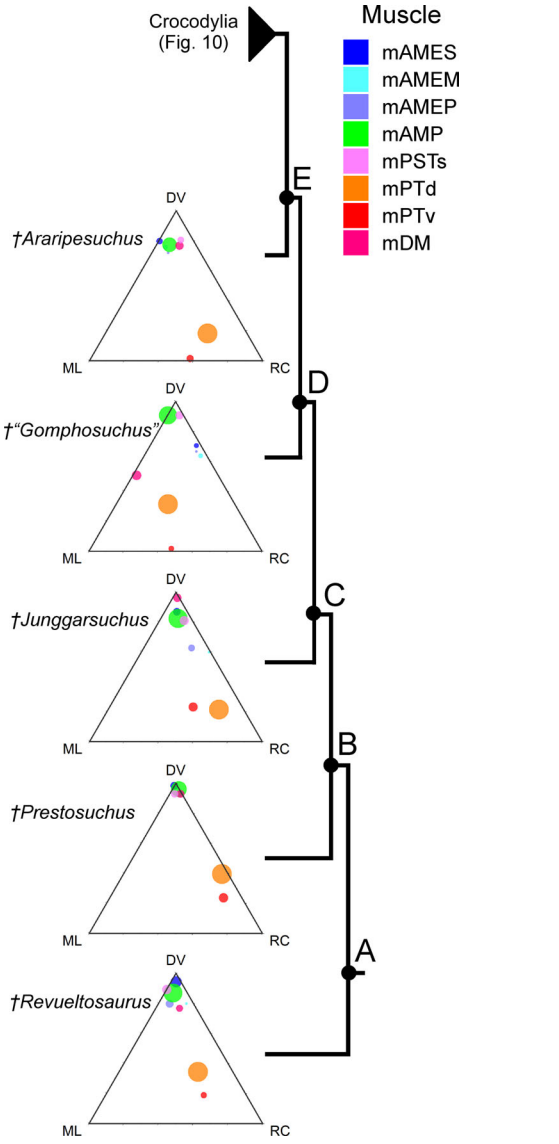

FIGURE 8 Ternary representation of jaw muscle evolution in the lineage leading to Crocodylia. Size of points indicates normalized muscle force. Note that muscles are clustered in the top corner of ternaries in basal taxa, indicating largely dorsoventrally oriented jaw muscles. (a) Suchia; (b) Loricata; (c) Crocodylomorpha; (d) Crocodyliformes; (e) Metasuchia. Extinct taxa are indicated with dagger symbol (†)

Numerous works have provided rich and detailed studies of the jaw musculature of extant crocodylian jaw muscles (Busbey, 1989; Holliday & Witmer, 2007; Iordansky, 1964; Schumacher, 1973), and although a thorough summary of their findings is beyond the scope of this paper, we briefly summarize the extant condition below. The rostral portions of the origin of mPTd have expanded to include the maxilla, nasal capsule, prefrontals, jugals, and even the ectopterygoids. This expanded origin is reflected in an enlarged insertion on the expanded articular bone. The insertion of m. pterygoideus ventralis (mPTv) has migrated onto the lateral surface of the mandible, leading this muscle to wrap ventromedially around the mandible. The origin of mPSTs does not lie within the dorsotemporal fenestra in extant crocodylians, as the laterosphenoid no longer participates in the fenestral margin, whereas the insertion of this muscle in extant crocodylians is equivalent to the intramandibularis (mIRA) muscle (Iordansky, 1964; Tsai & Holliday, 2011). The so-called "cartilago transiliens" is a sesamoid within mPSTs. mPSTs/ mIRA travels far rostrally within the primordial canal; in *Alligator*, the rostral extent is the crest that divides the canal for Meckel's cartilage from the canal for the inferior alveolar nerve (Lessner & Holliday, 2020). The origins of the mAME group are displaced by the diminished size of the dorsotemporal fenestra in crocodylians. Neither m. adductor mandibulae

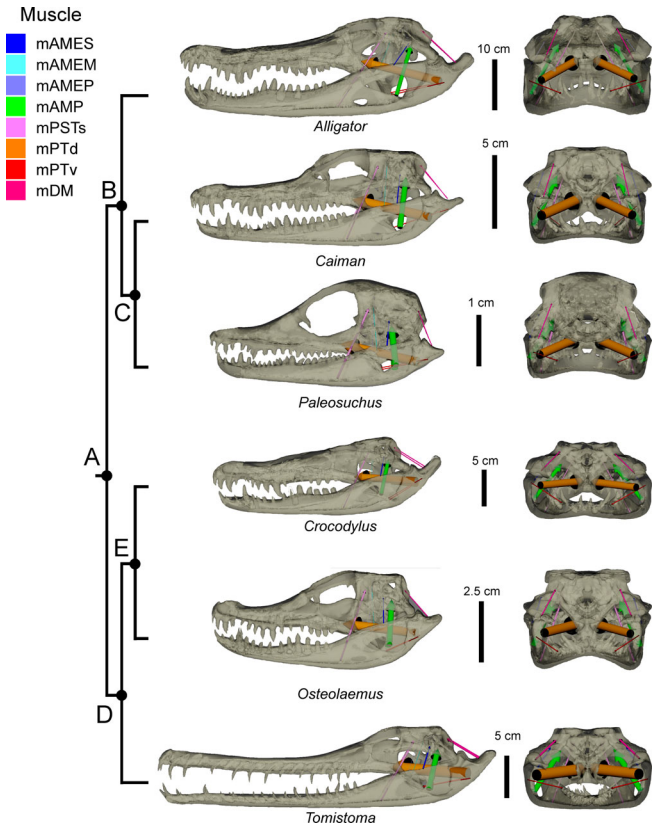

FIGURE 9 Jaw muscle anatomy is relatively conserved within Crocodylia but jaw muscles are still more oblique in animals with flatter skulls. Vector thickness and size of the matching point on ternary diagrams correspond to normalized muscle force. Models are scaled to the same skull height. (a) Crocodylia; (b) Alligatoridae; (c) Caimaninae; (d) Crocodylidae; (e) Crocodylinae. Crocodylinae then add Table A1 contains links to Sketchfab models of skulls with reconstructed muscle vectors

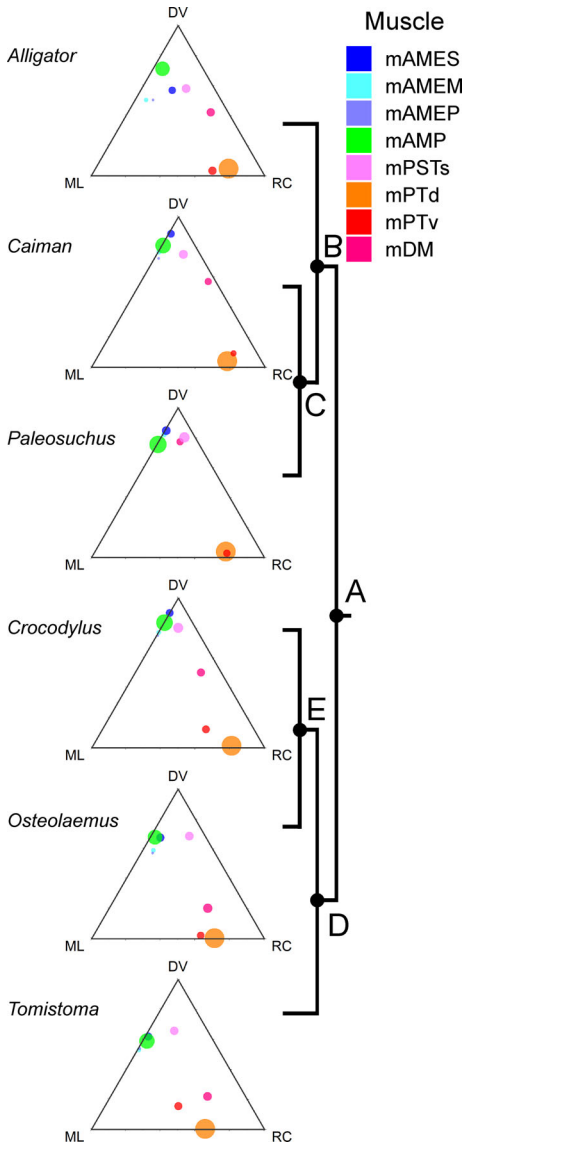

FIGURE 10 Ternary representation of jaw muscle orientation within Crocodylia. Size of points indicates normalized muscle force. (a) Crocodylia; (b) Alligatoridae; (c); Caimaninae; (d) Crocodylidae; (e) Crocodylinae

externus superficialis (mAMES) nor m. adductor mandibulae externus medialis (mAMEM) originate on the margin of the dorsotemporal fenestra; rather, both are displaced ventrally onto the quadrate and quadratojugal. The topographic relationships of mAMP are largely unchanged in crocodylians, but the development of a prominent tubercle on the quadrate reflects the presence of a central tendon (Adams et al., 2017; Hieronymus, 2006; Holliday, 2006). The m. depressor mandibulae is large and inserts onto an enlarged retroarticular process.

4.4 | Osteological correlates of muscle attachment in fossil suchians

4.4.1 | M. pterygoideus

The antorbital fenestra is closed in extant crocodylians, but soft tissue reconstructions suggest that the extensive pneumatic system of fossil archosaurs excavated the antorbital fossa and perforated the lateral wall of the rostrum, limiting the rostral extent of the origin of mPTd (Witmer, 1997). The shrinkage of the antorbital fenestra has thus been interpreted as an osteological correlate of the expansion of the origin of mPTd onto the nasal capsule, prefrontal, and maxilla in the vicinity of the caviconchal fossa (Witmer, 1997). The antorbital fossa and fenestra are diminished in "protosuchians" and most metasuchians; they are closed in most neosuchians. Thus, we reconstruct the expansion of the rostral origin of mPTd as taking place at the base of Crocodyliformes.

The insertion of mPTv extends onto the lateral surface of the mandible independently in numerous taxa as

evidenced by a clear and abrupt transition from sculptured to smooth texture. However, the muscle plesiomorphically attaches to the medial surface of the angular. In our sample, mPTv attaches on the lateral surface of the angular in *Junggarsuchus* (Ruebenstahl, 2019), *Araripesuchus* (Nieto et al., 2021), and all extant crocodylians, whereas *Revueltosaurus*, *Prestosuchus*, and "*Gomphosuchus*" lack a lateral insertion of mPTv. The distribution of a laterally inserting met is complex within Metasuchia. In basal notosuchians, a laterally inserting mPTv is present in the uruguaysuchid *A. gomesii* (present study) but absent from the uruguaysuchid *Uberabasuchus* (Carvalhol & Ribeirof, 2004). It is present in the peirosaurids *Mahajangasuchus* (Turner & Buckley, 2008) and *Kaprosuchus* (Sereno & Larsson, 2009) but absent in the peirosaurid *Montealosuchus* (Carvalho et al., 2007). It is absent from the basal ziphosuchian *Malawisuchus* (Gomani, 1997) but present in *Simosuchus* (Turner & Sertich, 2010). It is absent in most "advanced ziphosuchians" (Pol & Leardi, 2015); for example, *Mariliasuchus* (de Andrade & Bertini, 2008), *Notosuchus* (Fiorelli & Calvo, 2008), sphagesaurids (Pol et al., 2014), and sebecosuchians (Busbey, 1986; Kellner et al., 2014) but present in baurusuchids (Montefeltro et al., 2020). The muscle was also relegated to the medial and ventral mandible in many advanced neosuchians including goniopholids (Martin et al., 2020; Martin, Delfino, & Smith, 2016), pholidosaurs (Martin, Raslan-Loubatié, & Mazin, 2016), and paralligatorids (Turner, 2015). Basal eusuchians also lack the lateral insertion, including *Bernissartia* (Martin et al., 2020). The ubiquity of a laterally inserting mPTv in extant crocodylians suggests this trait is a synapomorphy of Crocodylia and that its absence in fossil crocodylians such as *Borealosuchus* (Brochu et al., 2012) resulted from secondary losses.

4.4.2 | M. pseudotemporalis

The dorsal skull table is contracted relative to the rest of the skull in metasuchians. In the non-metasuchian *Fruitachampsa* and the non-metasuchian mesoeucrocodylian *Pelagosaurus*, the lateral margin of the laterosphenoid is confluent with the dorsotemporal fenestra and the lateral margins of the skull table are directly dorsal to the jugals (Clark, 2011; Pierce & Benton, 2006). By contrast, in both basal notosuchians and neosuchians, the skull table is narrower than the skull as a whole and the dorsotemporal fenestrae are diminished. We thus reconstruct the exclusion of mPSTs from the dorsotemporal fenestra as originating in metasuchians. This is consistent with previous work on the temporal region of suchians (Holliday & Witmer, 2009).

4.4.3 | M. adductor mandibulae externus

In extant Crocodylia, the m. adductor mandibulae externus profundus (mAMEP) is the only muscle that occupies the dorsotemporal fenestra (Holliday et al., 2019; Holliday & Witmer, 2009). The origins of mAMEM and mAMES have been excluded from the fenestra and shifted onto the quadratojugal and quadrate. The shifts in mAME muscles were likely related to the narrow skull table of extant crocodylians. This trait first originated in Metasuchia. The shrinking of the dorsotemporal fenestra also had consequences for mPSTs, as discussed above.

4.4.4 | M. adductor mandibulae posterior

In extant Crocodylia, mAMP retains the ancestral attachments and is largely comparable to the ancestral condition, although its orientation is altered by shifts in skull geometry, as discussed below. The adductor tubercle of the attachment of the central tendon of mAMP (Iordansky, 1964) dates to at least Eusuchia (Holliday & Gardner, 2012; Narváez et al., 2015).

4.4.5 | M. depressor mandibulae

Most notosuchians and neosuchians show some form of retroarticular process. The characteristic elongate retroarticular process increases the maximum moment arm available for fibers of mDM. An elongate retroarticular process also provides an enlarged moment arm for portions of mPTd (Gignac & O'Brien, 2016), although the majority of the insertion is not affected by the retroarticular process. Although most "protosuchians" lack this retroarticular process, basal crocodylomorphs close to the ancestry of Crocodyliformes (e.g., *Junggaruschus* and *Almadasuchus*) constructed a similar process (Pol et al., 2013), suggesting an apomorphic loss in "Protosuchia." All crocodyliforms show a reduced posttemporal fenestra (Busbey & Gow, 1984; Iordansky, 1973), providing a larger surface for the origin of mDM. Thus, we reconstruct an expanded mDM as ancestral for Crocodyliformes. Some "protosuchians" (e.g., *Protosuchus*, "*Gomphosuchus*") reduced the retroarticular process and evolved an accompanying medial process of the articular (Wu et al., 1994), effectively shifting the insertion of mDM medially. Some shartegosuchoids, which are either "protosuchians" or basal mesoeucrocodylians, show a ventrally angled retroarticular process (Clark, 2011; Wu et al., 1997). This derived mDM morphology may be linked with the active oral processing of plant matter in which "*Gomphosuchus*"

probably engaged. Ősi (2014) reported that the worn, bicuspid teeth of "*Gomphosuchus*" are highly indicative of active oral processing of plant matter. If significant mandibular translational movements were a feature of the power stroke during "*Gomphosuchus*" feeding, an accompanying modification may be expected in the jaw depressors to counter or reverse this translation, but this hypothesis remains to be tested.

4.5 | Quantitative reconstructions

Muscle force is dominated by the pterygoideus muscles, with mPTd and mPTv together accounting for ~40%–50% of gross muscle force (Figure 6; Tables 2 and 3). Adductor mandibulae posterior is the second largest muscle, accounting for ~25%–30% (Figure 6; Tables 2 and 3). Proportions of muscle force are surprisingly consistent across the sample in light of previous hypothesized relationships between the size of the dorsotemporal fenestra and muscle mass, although recent work has called into question the utility of dorsotemporal fenestra size and muscle anatomy (Holliday et al., 2019). Adductor mandibulae externus muscles accounts for a slightly higher proportion of gross muscle force in early suchians (Figure 6; Tables 2 and 3), and within extant crocodylians, the pterygoideus muscles contribute a larger proportion of muscle force in larger individuals, consistent with previously-reported data on muscle scaling in crocodylians (Gignac & Erickson, 2016).

Muscle forces are generally less dorsoventrally oriented in crocodylians than in extinct suchians (Figures 7–10). Temporal muscles in extant taxa are generally ~10% less dorsoventrally oriented than the same muscles in fossil taxa (Figures 7–10). Differences in orientations of the pterygoideus muscles are even more dramatic: mPTd is ~25% dorsoventrally oriented in fossil taxa, whereas it is nearly in the horizontal plane in extant taxa at ~10% dorsoventrally oriented (Figures 7–10; Table S1). Finally, mDM is nearly 30% less dorsoventrally oriented in extant taxa than in extinct taxa (Figures 7–10).

4.6 | Gross muscle force, muscle resultant, and muscle efficiency

Magnitudes of both gross muscle force and resultant muscle force were strongly linked with size. Gross muscle force ranged from a low of 202 N in *Paleosuchus* to a high of 29,100 N in *Alligator* (Table 4). The magnitude of the muscle resultant ranged from 138 N in *Paleosuchus* to a high of 20,200 N in *Prestosuchus* (Table 4). Muscle efficiency (i.e., the ratio of resultant muscle force and gross muscle force) ranged from ~0.53 in *Crocodylus* and ~0.56 in *Tomistoma* to ~0.86 in *Prestosuchus* (Figure 11). Thus, nearly 60% more of the available jaw muscle force is realized as muscle resultant force in *Prestosuchus* than in *Crocodylus*.

4.7 | Hypothesis testing

Our analyses show that skull size and skull flatness both jointly influence muscle performance. Gross muscle force was best explained by skull size (i.e., PC1) alone, whereas resultant muscle force was best explained by skull size and skull flatness (i.e., PC1 + PC2). Hypothesis 1 was therefore supported. The relationship between muscle efficiency and skull flatness (i.e., PC2) was significant, supporting Hypothesis 2. There was no relationship between gross muscle force and PC2, failing to support Hypothesis 3A. There was no relationship between the sum of moment arms and PC2, failing to support Hypothesis 3B (Table 5).

5 | DISCUSSION

5.1 | The effects of skull flattening

Skull flattening is a major feature of crocodylian evolution (Busbey, 1995; Cossette, 2018; Langston, 1973). Numerous derived traits contribute to the complex morphology of skull flattening, including the caudolateral rotation of the quadrate condyles (Busbey, 1995; Langston, 1973), formation of the "skull table" (Busbey, 1995; Cossette, 2018; Langston, 1973), and rostral flattening (Busbey, 1995). Functional explanations of crocodylian skull flattening have focused on presumed adaptations to aquatic ambush predation, such as the dorsal migration of the sensory structures allowing crocodylians to float nearly submerged (Cossette, 2018; Iordansky, 1973; Langston, 1973) or reducing drag during lateral head movements (Busbey, 1995; McHenry et al., 2006).

Although the development of high bite force performance likely played a large role in crocodylian evolution (Langston, 1973), our analyses found that the crocodylian adductor chamber is not optimized for the efficient production of high bite force, as extant crocodylians had lower values of muscle efficiency than fossil suchians (Table 4). Other studies have shown that the geometry of the crocodylian rostrum is not optimized for the resistance of dorsoventral bending or twisting loads (Busbey, 1995; McHenry et al., 2006; Metzger et al., 2005). This suggests that conflicting functional demands played roles in crocodylian skull shape evolution. Authors have noted that derived traits in the

TABLE 2 Proportion of jaw gross muscle force represented by each muscle belly

	Jaw muscle bellies							
Genus	**mAMES**	**mAMEM**	**mAMEP**	**mAMP**	**mPSTs**	**mPTd**	**mPTv**	**mDM**
Alligator	4.5%	1.4%	0.79%	23.9%	7.1%	50.1%	6.2%	6.0%
Caiman	5.0%	1.7%	0.91%	28.5%	7.5%	49.5%	2.7%	4.3%
Paleosuchus	6.0%	2.1%	1.1%	31.0%	9.5%	42.3%	4.1%	4.0%
Crocodylus	5.2%	1.1%	0.6%	26.4%	6.1%	48.6%	5.5%	6.5%
Osteolaemus	4.8%	1.6%	1.00%	29.5%	8.9%	44.2%	4.9%	5.2%
Tomistoma	5.9%	1.6%	0.98%	24.4%	6.8%	47.7%	4.8%	7.9%
Araripesuchus[a]	3.3%	1.8%	0.98%	25.7%	3.7%	53.4%	4.6%	6.5%
"*Gomphosuchus*"[a]	3.1%	3.2%	2.5%	32.9%	6.4%	39.8%	3.5%	8.7%
Junggarsuchus[a]	4.4%	1.2%	3.3%	34.4%	6.6%	38.2%	6.6%	5.3%
Prestosuchus[a]	6.0%	2.2%	3.6%	25.8%	5.4%	42.6%	8.5%	6.0%
Revueltosaurus[a]	10.3%	1.7%	4.8%	32.8%	6.9%	36.7%	3.1%	3.8%

[a]Extinct taxa.

TABLE 3 Forces in newtons produced by each jaw muscle belly

	Jaw muscle bellies							
Genus	**mAMES**	**mAMEM**	**mAMEP**	**mAMP**	**mPSTs**	**mPTd**	**mPTv**	**mDM**
Alligator	660	197	115.5	3,475	1,035	7,300	905	875
Caiman	35.2	12.2	6.45	201.5	53	350	19.0	30.4
Paleosuchus	6.1	2.1	1.06	31.25	9.55	42.65	4.2	4.0
Crocodylus	262.5	53.5	31.2	1,335	307.5	2,450	276.5	326.5
Osteolaemus	24.7	8.1	5.15	151	45.5	226.5	25.1	26.8
Tomistoma	236.5	62.5	39.1	975	273	1900	191.5	313
Araripesuchus[a]	15.5	8.6	4.62	121	17.4	251.5	21.5	30.6
"*Gomphosuchus*"[a]	6.35	6.4	5.1	67	13.05	81	7.2	17.6
Junggarsuchus[a]	34.2	9.75	25.9	271	51.5	300.5	51.5	42
Prestosuchus[a]	710	262	423	3,045	640	5,050	1,005	705
Revueltosaurus[a]	149	24.6	70.5	476.5	100	535	44.6	55.5

[a]Extinct taxa.

crocodylian rostrum such as a bony secondary palate and broad scarf joints at least partially compensate for the structural inefficiency imposed by a flattened skull (Busbey, 1989; Busbey, 1995; McHenry et al., 2006; Metzger et al., 2005; Porro et al., 2011), and derived aspects of the crocodylian jaw adductors (especially the evolutionary hypertrophy of the pterygoideus muscles) may similarly mitigate the functional consequences of inefficient muscle geometry caused by the flat skull (Salisbury et al., 2006; Gignac & Erickson, 2016; Gignac & O'Brien, 2016; see below).

Some authors have noted ontogenetic and phylogenetic "verticalization" of the braincase of crocodylians and other derived neosuchians (Salisbury et al., 2006; Tarsitano, 1985). Changes to the basisphenoid and basioccipital result in a more dorsoventrally tall braincase. These authors suggested that braincase verticalization may result in *more* dorsoventrally oriented jaw muscles relative to primitive neosuchians, although these studies did not perform quantitative reconstruction of jaw muscle anatomy. In contrast, this study found the temporal and pterygoideus muscles reoriented to more horizontal orientation despite this pattern of braincase verticalization. This suggests that the braincase, palate, and skull roof elements may have evolved as separate modules, consistent with previous work (Felice et al., 2019).

Eusuchians including Crocodylia inherited flat skulls from a bottleneck of skull flatness around the base of Neosuchia. The most basal neosuchians such as *Goniopholis* (de Andrade et al., 2011), *Bernissartia* (Martin

TABLE 4 Gross muscle force, muscle resultant, and muscle efficiency among suchian sample

Genus	Gross muscle force (F_g; N)	Muscle resultant (F_r; N)	Muscle efficiency
Alligator	29,100	17,700	0.608
Caiman	1,420	939	0.663
Paleosuchus	202	138	0.684
Crocodylus	10,100	5,360	0.531
Osteolaemus	1,030	662	0.646
Tomistoma	7,980	4,460	0.559
Araripesuchus[a]	941	671	0.713
"*Gomphosuchus*"[a]	407	305	0.750
Junggarsuchus[a]	1,570	1,150	0.729
Prestosuchus[a]	23,700	20,200	0.855
Revueltosaurus[a]	2,910	2,350	0.809

[a]Extinct taxa.

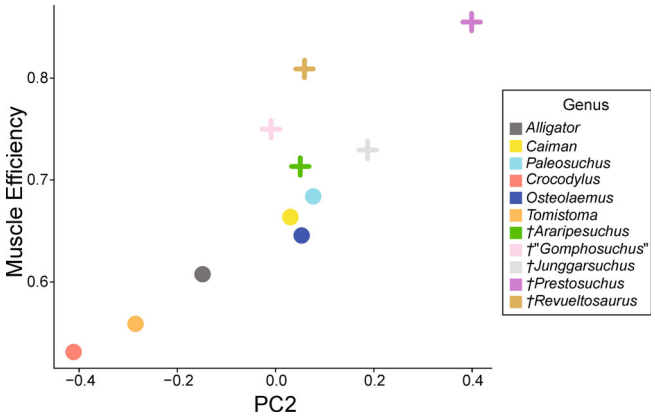

FIGURE 11 Muscle efficiency in fossil suchians is higher than in crocodylians and is inversely related to skull flatness. Extinct taxa are indicated with dagger symbol (†)

et al., 2020; Norell & Clark, 1990), and stomatosuchids including *Stomatosuchus* and *Laganosuchus* (Sereno & Larsson, 2009) showed some of the flattest skulls from the suchian record. This trend continued into Eusuchia as documented by *Isisfordia* (Salisbury et al., 2006), *Iharkutosuchus* (Ősi, 2008; Ősi et al., 2007) and aegyptosuchids (Holliday & Gardner, 2012). Some eusuchians including *Isisfordia* and Crocodylia extended the pterygoid flange ventrally (Salisbury et al., 2006), which increases the available attachment area for m. pterygoideus ventralis and permits a larger mPTd to course dorsal to this element. Additionally, the cranial attachment of m. adductor mandibulae posterior develops an enlarged adductor tubercle suggestive of increased tendinous attachment. This likely reflects a packing of a larger number of shorter muscle fascicles, increasing the force this muscle produces. Thus, the appearance of elaborate crests and tubercles on the quadrate of eusuchians helps to offset the inefficient muscle orientations inherited from neosuchians and serves as further evidence that derived suchians rely on increasing muscle mass to facilitate the generation of bite force.

In addition, this analysis shows signs of ontogenetic recapitulation. Although the focus of this study was a comparison among taxa, smaller extant crocodylians had more dorsoventrally oriented muscles. This matches findings from an ontogenetic sample of *A. mississippiensis* (Cost et al., 2022). Heterochronic shifts are a common source of evolutionary shape change, and have been suggested to underlie other aspects of crocodylian skull shape and functional evolution (Gignac & O'Brien, 2016; Morris et al., 2019).

5.2 | Evolution of pterygoideus musculature

The pterygoid muscles have been considered to be key characters in the evolution of the crocodylian feeding apparatus (Gignac & Erickson, 2016; Gignac & O'Brien, 2016; Holliday & Witmer, 2007; Iordansky, 1964, 2010; Salisbury et al., 2006). Previous work has implicated the ventral deflection of the pterygoid flanges in neosuchians in increasing the size of mPTd (Salisbury et al., 2006) and relative size of the jaw adductors (Iijima, 2017). In extant crocodylians, mPTv is especially well suited to increasing its size, as mPTv is uniquely not bound by the bony adductor chamber (Gignac et al., 2019; Salisbury et al., 2006) and has extensive tendinous origins (Busbey, 1989; Holliday & Witmer, 2007, 2009; Iordansky, 1964, 2010; Schumacher, 1973). This lack of osteological correlates makes predicting the size (mass, volume) of these muscles challenging. The complex internal anatomy of mPTv and its wrapping geometry also make it difficult to accurately model with traditional approaches (Gignac & Erickson, 2016; Sellers et al., 2017), and previous studies in extant crocodylians have reported widely different proportions of the pterygoid muscles relative both to each other and to other jaw muscles (Busbey, 1989: mPTd ~18%, mPTv ~34%; Cleuren et al., 1995: mPTd ~18%, mPTv ~34%; Porro et al., 2011: mPTd ~47%, mPTV ~20%; Gignac & Erickson, 2016: mPTd ~17%, mPTv ~62%). In our quantitative reconstructions, mPTd in crocodylians ranged from ~50% of gross muscle force in *Alligator* to ~42% in *Paleosuchus*, and mPTv ranged from ~6% in *Alligator* and *Crocodylus* to ~3% in *Paleosuchus*. Among the whole suchian sample, mPTd ranged from ~50% in *Alligator* to ~37% in *Revueltosaurus*, and mPTv ranged from ~6% in *Alligator* and *Crocodylus* to ~3% in *Paleosuchus*. We tentatively hypothesize that an attachment of mPTv on the lateral

TABLE 5 Results of statistical analyses

Mod.	Resp. Var.	Pred. Var(s).	β_1	p_1	β_2	p_2	AICc	AICw
1.1	F_r	PC1	−5,247 ± 343.3	<.001	N/A	N/A	207.5	0.04
1.2	F_r	PC2	17,029 ± 13,218	.230	N/A	N/A	241.8	0.00
1.3	**F_r**	**PC1 + PC2**	**−5,033 ± 219.3**	<.001	**6,967 ± 1,770**	**.004**	**200.8**	**0.96**
2.1	E_M	PC1	−0.0160 ± 0.018	.387	N/A	N/A	−8.92	0.00
2.2	**E_M**	**PC2**	**0.387 ± 0.086**	**.0015**	**N/A**	**N/A**	**−20.88**	**0.92**
2.3	E_M	PC1 + PC2	−0.0051 ± 0.0115	.667	0.376 ± 0.093	.004	−15.92	0.08
3.1	**F_g**	**PC1**	**−6,501 ± 339.5**	**<.001**	**N/A**	**N/A**	**207.2**	**0.92**
3.2	F_g	PC2	14,436 ± 17,039	.419	N/A	N/A	247.4	0.00
3.3	F_g	PC1 + PC2	−6,454 ± 365.6	<.001	1,533 ± 2,951	.618	212.1	0.08
3.4	**$\sum l_m$**	**PC1**	**−0.260 ± 0.0052**	**<.001**	**N/A**	**N/A**	**−36.38**	**0.74**
3.5	$\sum l_m$	PC2	0.5808 ± 0.673	.411	N/A	N/A	24.35	0.00
3.6	$\sum l_m$	PC1 + PC2	−0.2578 ± 0.0050	<.001	0.065 ± 0.040	.145	−34.24	0.26

Note: For hypotheses with multiple significant models, the best-fit model is bolded.
Abbreviations: $\sum l_m$, sum of moment arms; AICc, Akaike information criterion corrected for small sample size; AICw, AICc weights; β_1, effect of the first variable ±95% confidence interval; β_2, effect of the second variable ± standard error; Mod., model number; p_1, p value of first variable; p_2, p value of second variable; Pred. Var(s)., predictor variable(s); Resp. Var., response variable.

mandible, as found in all extant crocodylians, may be an osteological correlate of a hypertrophied mPTd displacing the insertion of mPTv laterally.

The distribution of a laterally attaching pterygoideus ventralis among crocodylomorphs suggests rampant homoplasy. The distribution of a laterally attaching mPTv suggests this muscle migrated onto the lateral surface of the mandible independently late in the lineage leading to Crocodylia and near the base of Notosuchia, followed by a subsequent loss in numerous notosuchians. Alternatively, a laterally attaching mPTv may be basal for Metasuchia, although this would require numerous losses within both Neosuchia and Notosuchia. Taxa just outside of Eusuchia such as *Isisfordia* (Salisbury et al., 2006) shifted the pterygoid flange ventrally, both widening the space available for mPTd and increasing the attachment area of mPTv. As the flat skull predates the persistent lateral insertion of mPTv in the crown clade, we suggest that the evolutionary hypertrophy of mPT facilitates high bite force performance despite the geometric inefficiencies imposed by the skull flattening for aquatic ambush predation.

This study highlights the diversity and evolution of jaw muscles in suchians during one of the great transformations in vertebrate evolution. Although many studies have focused on the evolution of shape in the suchian feeding apparatus (Drumheller & Wilberg, 2020; Pierce et al., 2009; Stubbs et al., 2021) and the response of the feeding apparatus to forces (McHenry et al., 2006; Walmsley et al., 2013), less attention has been paid to the jaw muscles driving feeding function (but see Schumacher, 1973; Porro et al., 2011, 2013; Ősi, 2014; Gignac & O'Brien, 2016). The reconstruction of jaw muscle evolution presented here clarifies and constrains future functional studies of feeding in Suchia.

6 | CONCLUSIONS

Here, we reconstruct jaw musculature in a sample of suchians leading to the crown group. Muscle proportions show surprising conservatism across the sample, but muscles are in less efficient configurations in extant taxa that possess flat skulls. We found no evidence of taxa with flatter skulls relying on larger gross muscle mass or longer moment arms of muscles to mitigate inefficient muscular geometries. Future studies will analyze the effects of inefficient muscular geometries on feeding performance and evolution.

AUTHOR CONTRIBUTIONS

Kaleb C. Sellers: Conceptualization (lead); formal analysis (lead); funding acquisition (supporting); investigation (lead); methodology (lead); visualization (lead); writing – original draft (lead); writing – review and editing (lead). **Mauro Nicolas Nieto:** Formal analysis (supporting); investigation (supporting); methodology (supporting); writing – original draft (supporting); writing – review and editing (supporting). **Federico J. Degrange:** Investigation (supporting); methodology (supporting); writing – original draft (supporting); writing – review and editing (supporting). **Diego Pol:** Funding acquisition (supporting); investigation (supporting); methodology (supporting); writing –

original draft (supporting); writing – review and editing (supporting). **James M. Clark:** Funding acquisition (lead); investigation (supporting); methodology (supporting); writing – original draft (supporting); writing – review and editing (supporting). **Kevin M. Middleton:** Investigation (supporting); methodology (supporting); visualization (supporting); writing – original draft (supporting); writing – review and editing (supporting). **Casey M. Holliday:** Conceptualization (supporting); funding acquisition (lead); investigation (supporting); methodology (supporting); visualization (supporting); writing – original draft (supporting); writing – review and editing (supporting).

ACKNOWLEDGMENTS

This study was supported by the National Science Foundation (NSF-EAR 1631684 and 1636753), the Society of Vertebrate Paleontology, the University of Missouri Research Board, the University of Missouri Research Council, Agencia Nacional de Promoción Científica y Tecnológica, and CONICET. The authors would like to thank Ruth Elsey and the staff at the Rockefeller Wildlife Refuge for providing alligator specimens. They also thank field crews and museum curators for access to specimens. Fieldwork on the Navajo Nation was conducted under a permit from the Navajo Nation Minerals Department. Any persons wishing to conduct geologic investigations on the Navajo Nation must first apply for and receive a permit from the Navajo Nation Minerals Department, P.O. Box 1910, Window Rock, Arizona 86515, and telephone no.: (928) 871-6587. Special thanks to Cesar Shultz, Alex Liparini, Adam Marsh, Alex Ruebenstahl, and Bill Parker for providing imaging data for fossil species.

ORCID

Kaleb C. Sellers https://orcid.org/0000-0002-3588-9562
Federico J. Degrange https://orcid.org/0000-0002-9463-4893
Kevin M. Middleton https://orcid.org/0000-0003-4704-1064
Casey M. Holliday https://orcid.org/0000-0001-8210-8434

REFERENCES

Adams, T. L., Noto, C. R., & Drumheller, S. (2017). A large neosuchian crocodyliform from the upper cretaceous (Cenomanian) woodbine formation of North Texas. *Journal of Vertebrate Paleontology*, *37*, e1349776.

Bates, K. T., & Falkingham, P. L. (2018). The importance of muscle architecture in biomechanical reconstructions of extinct animals: a case study using *Tyrannosaurus rex*. *Journal of Anatomy*, *223*, 625–635.

Brazeau, M. D., Friedman, M., Jerve, A., & Atwood, R. (2017). A three-dimensional placoderm (stem-group gnathostome) pharyngeal skeleton and its implications for primitive gnathostome pharyngeal architecture. *Journal of Morphology*, *278*, 1220–1228.

Brochu, C. A. (2001). Crocodylian snouts in space and time: Phylogenetic approaches toward adaptive radiation. *American Zoologist*, *41*, 564–585.

Brochu, C. A., Parris, D. C., Grandstaff, B. S., Denton, R. K., Jr., Gallagher, W. B., & Taylor, P. (2012). A new species of *Borealosuchus* (Crocodyliformes, Eusuchia) from the Late Cretaceous–early Paleogene of New Jersey. *Journal of Vertebrate Paleontology*, *32*, 105–116.

Busbey, A. B. (1986). New material of *Sebecus* cf. *huilensis* (Crocodilia: Sebecosuchidae) from the Miocene La Venta formation of Colombia. *Journal of Vertebrate Paleontology*, *6*, 20–27.

Busbey, A. B. (1989). Form and function of the feeding apparatus of *Alligator mississippiensis*. *Journal of Morphology*, *202*, 99–127.

Busbey, A. B. (1995). The structural consequences of skull flattening in crocodilians. In *Functional morphology in vertebrate paleontology* (pp. 173–192). Cambridge University Press.

Busbey, A. B., & Gow, C. (1984). A new protosuchian crocodile from the upper Triassic Elliot formation of South Africa. *Palaeotologia Africana*, *25*, 127–149.

Carvalho, I. D. E. S., Vasconcellos, F. M. D. E., & Simionato Tavares, S. A. (2007). *Montealtosuchus arrudacamposi*, a new peirosaurid crocodile (Mesoeucrocodylia) from the Late Cretaceous Adamantina formation of Brazil. *Zootaxa*, *46*, 35–46.

Carvalhol, I. D. S., & Ribeirof, L. C. B. (2004). *Uberabasuchus terrificus sp. nov*., a new Crocodylomorpha from the Bauru Basin (upper cretaceous), Brazil. *Gondwana Res*, *7*, 975–1002.

Cidade, G. M., Fortier, D., & Hsiou, A. S. (2019). The crocodylomorph fauna of the Cenozoic of South America and its evolutionary history: a review. *Journal of South American Earth Sciences*, *90*, 392–411.

Clark, J. M. (1986). *Phylogenetic relationships of the Crocodylomorph archosaurs* (PhD dissertation). University of Chicago.

Clark, J. M. (2011). A new shartegosuchid crocodyliform from the upper Jurassic Morrison formation of western Colorado. *Zoological Journal of the Linnean Society*, *163*, 152–172.

Clark, J. M., Xu, X., Forster, C. A., & Wang, Y. (2004). A middle Jurassic "sphenosuchian" from China and the origin of the crocodylian skull. *Nature*, *430*, 1021–1024.

Clausen, P. D., Wroe, S., McHenry, C. R., Moreno, K., & Bourke, J. (2008). The vector of jaw muscle force as determined by computer-generated three dimensional simulation: A test of Greaves' model. *Journal of Biomechanics*, *41*, 3184–3188.

Cleuren, J., Aerts, P., & De Vree, F. L. (1995). Bite and joint force analysis in *Caiman crocodilus*. *Belgian Journal of Zoology*, *125*, 79–94.

Cossette, A. P. (2018). *The early history of character evolution in alligatoroids* (PhD dissertation). University of Iowa.

Cost, I. N., Middleton, K. M., Sellers, K. C., Echols, M. S., Witmer, L. M., Davis, J. L., & Holliday, C. M. (2020). Palatal biomechanics and its significance for cranial kinesis in *tyrannosaurus rex*. *The Anatomical Record*, *303*, 999–1017.

Cost, I. N., Sellers, K. C., Rozin, R. E., Spates, A. T., Middleton, K. M., & Holliday, C. M. (2022). 2D and 3D visualizations of archosaur jaw muscle mechanics, ontogeny, and phylogeny using ternary diagrams and 3D modeling. *The Journal of Experimental Biology*, *225*, jeb243216.

Cox, P. G., Rayfield, E. J., Fagan, M. J., Herrel, A., Pataky, T. C., & Jeffery, N. (2012). Functional evolution of the feeding system in rodents. *PLoS One*, *7*, e36299.

Davis, J. L., Santana, S. E., Dumont, E. R., Grimwood, J., & Grosse, I. R. (2010). Predicting bite force in mammals: Two-dimensional versus three-dimensional lever models. *The Journal of Experimental Biology*, *213*, 1844–1851.

de Andrade, M. B., & Bertini, R. (2008). Morphological and anatomical observations about *Mariliasuchus amarali* and *Notosuchus terrestris* (Mesoeucrocodylia) and their relationships with other South American notosuchians. *Arquivos do Museu Nacional*, *66*(1), 5–62.

de Andrade, M. B., Edmonds, R., Benton, M. J., & Schouten, R. (2011). A new Berriasian species of Goniopholis (Mesoeucrocodylia, Neosuchia) from England, and a review of the genus. *Zoological Journal of the Linnean Society*, *163*, S66–S108.

Drumheller, S. K., & Wilberg, E. W. (2020). A synthetic approach for assessing the interplay of form and function in the crocodyliform snout. *Zoological Journal of the Linnean Society*, *188*, 507–521.

Dumont, E. R., Herrel, A., Medellí-n, R. A., Vargas-Contreras, J. A., & Santana, S. E. (2009). Built to bite: Cranial design and function in the wrinkle-faced bat. *Journal of Zoology*, *279*, 329–337.

Erickson, G. M., Lappin, A. K., & Vliet, K. A. (2003). The ontogeny of bite-force performance in American alligator (*Alligator mississippiensis*). *Journal of Zoology*, *260*, 317–327.

Felice, R. N., Watanabe, A., Cuff, A. R., Noirault, E., Pol, D., Witmer, L. M., Norell, M. A., O'Connor, P. M., & Goswami, A. (2019). Evolutionary integration and modularity in the archosaur cranium. *Integrative and Comparative Biology*, *59*, 371–382.

Fiorelli, L. E., & Calvo, J. (2008). New remains of *Notosuchus terrestris* Woodward, 1896 (Crocodyliformes: Mesoeucrocodylia) from late cretaceous of Neuquén, Patagonia, Argentina. *Arquivos do Museu Nacional*, *66*, 83–124.

Fish, F. E., Bostic, S. A., Nicastro, A. J., & Beneski, J. T. (2007). Death roll of the alligator: Mechanics of twist feeding in water. *The Journal of Experimental Biology*, *210*, 2811–2818.

Gans, C. (1989). Stages in the origin of vertebrates: Analysis by means of scenarios. *Biological Reviews of the Cambridge Philosophical Society*, *64*, 221–268.

Gans, C., & Northcutt, R. G. (1983). Neural crest and the origin of vertebrates: a new head. *Science*, *220*, 268–273.

Gignac, P. M., & Erickson, G. M. (2016). Ontogenetic bite-force modeling of *Alligator mississippiensis*: Implications for dietary transitions in a large-bodied vertebrate and the evolution of crocodylian feeding. *Journal of Zoology*, *299*, 229–238.

Gignac, P. M., & O'Brien, H. D. (2016). Suchian feeding success at the Interface of ontogeny and macroevolution. *Integrative and Comparative Biology*, *icw041*, 449–458.

Gignac, P. M., O'Brien, H. D., Turner, A. H., & Erickson, G. M. (2019). Feeding in Crocodylians and their relatives: Functional insights from ontogeny and evolution. In V. Bels & I. Q. Whishaw (Eds.), *Feeding in Vertebrates* (pp. 575–610). Springer.

Gomani, E. M. (1997). A crocodyliform from the early cretaceous dinosaur beds, northern Nalawi. *Journal of Vertebrate Paleontology*, *17*, 280–294.

Granatosky, M. C., & Ross, C. F. (2020). Differences in muscle mechanics underlie divergent optimality criteria between feeding and locomotor systems. *Journal of Anatomy*, *237*, 1–15.

Greaves, W. S. (1978). The jaw lever system in ungulates: a new model. *Journal of Zoology*, *184*, 271–285.

Greaves, W. S. (1982). A mechanical limitation on the position of the jaw muscles of mammals: The one-third rule. *Journal Of Mammology*, *63*, 261–266.

Greaves, W. S. (2000). Location of the vector of jaw muscle force mammals. *Journal of Morphology*, *243*, 293–299.

Hamilton, N. E., & Ferry, M. (2018). Ggtern: Ternary diagrams using ggplot2. *Journal of Statistical Software*, *87*, 1–17.

Herrel, A., De Grauw, E., & Lemos-Espinal, J. A. (2001). Head shape and bite performance in xenosaurid lizards. *The Journal of Experimental Zoology*, *290*, 101–107.

Herrel, A., Podos, J., Huber, S. K., & Hendry, A. P. (2005). Evolution of bite force in Darwin's finches: A key role for head width. *Journal of Evolutionary Biology*, *18*, 669–675.

Hieronymus, T. L. (2006). Quantitative microanatomy of jaw muscle attachment in extant Diapsids. *Journal of Morphology*, *267*, 954–967.

Holliday, C. M. (2006). Evolution and function of the jaw musculature and adductor chamber of archosaurs (crocodilians, dinosaurs, and birds) (PhD dissertation). University of Ohio.

Holliday, C. M., & Gardner, N. M. (2012). A new eusuchian crocodyliform with novel cranial integument and its significance for the origin and evolution of crocodylia. *PLoS One*, *7*, e30471.

Holliday, C. M., Porter, W. R., Vliet, K. A., & Witmer, L. M. (2019). The Frontoparietal fossa and Dorsotemporal fenestra of archosaurs and their significance for interpretations of vascular and muscular anatomy in dinosaurs. *The Anatomical Record*, *303*, 1060–1074.

Holliday, C. M., & Witmer, L. M. (2007). Archosaur adductor chamber evolution: Integration of musculoskeletal and topological criteria in jaw muscle homology. *Journal of Morphology*, *268*, 457–484.

Holliday, C. M., & Witmer, L. M. (2009). The Epipterygoid of Crocodyliforms and its significance for the evolution of the Orbitotemporal region of Eusuchians. *Journal of Vertebrate Paleontology*, *29*, 715–733.

Huber, D. R., Dean, M. N., & Summers, A. P. (2008). Hard prey, soft jaws and the ontogeny of feeding mechanics in the spotted ratfish *Hydrolagus colliei*. *Journal of the Royal Society Interface*, *5*, 941–952.

Hylander, W. L. (1975). The human mandible: Lever or link? *American Journal of Physical Anthropology*, *43*, 227–242.

Iijima, M. (2017). Assessment of trophic ecomorphology in non-alligatoroid crocodylians and its adaptive and taxonomic implications. *Journal of Anatomy*, *231*, 192–211.

Iordansky, N. N. (1964). The jaw muscles of the crocodiles and some relating structures of the crocodilian skull. *Anatomischer Anzeiger*, *115*, 256–280.

Iordansky, N. N. (1973). The skull of the Crocodilia. In C. Gans (Ed.), *Biology of the Reptilia* (Vol. 4, pp. 201–261). Academic Press.

Iordansky, N. N. (2010). Pterygoideus muscles and other jaw adductors in amphibians and reptiles. *The Biological Bulletin*, *37*, 905–914.

Kellner, A. W. A., Pinheiro, A. E. P., & Campos, D. A. (2014). A new sebecid from the paleogene of Brazil and the crocodyliform radiation after the K-pg boundary. *PLoS One*, *9*, e81386.

Langston, W. J. (1973). The crocodilian skull in historical perspective. In C. Gans (Ed.), *Biology of the Reptilia* (Vol. 4, pp. 263–284). Academic Press.

Lauder, G. V. (1995). On the inference of function from structure. In J. J. Thomason (Ed.), *Functional morphology in vertebrate paleontology* (pp. 1–18). Cambridge University Press.

Lessner, E. J., & Holliday, C. M. (2020). A 3D ontogenetic atlas of *Alligator mississippiensis* cranial nerves and their significance for comparative neurology of reptiles. *The Anatomical Record*, *305*(10), 2854–2882.

Martin, J. E., Delfino, M., & Smith, T. (2016). Osteology and affinities of Dollo's goniopholidid (Mesoeucrocodylia) from the early cretaceous of Bernissart, Belgium. *Journal of Vertebrate Paleontology*, *36*, e1222534.

Martin, J. E., Raslan-Loubatié, J., & Mazin, J. M. (2016). Cranial anatomy of *Pholidosaurus purbeckensis* from the lower cretaceous of France and its bearing on pholidosaurid affinities. *Cretaceous Research*, *66*, 43–59.

Martin, J. E., Smith, T., Salaviale, C., Adrien, J., & Delfino, M. (2020). Virtual reconstruction of the skull of *Bernissartia fagesii* and current understanding of the neosuchian–eusuchian transition. *Journal of Systematic Palaeontology*, *18*, 1079–1101.

Maynard-Smith, J., & Savage, R. (1959). The mechanics of mammalian jaws. *School Science Review*, *141*, 289–301.

McHenry, C. R., Clausen, P. D., Daniel, W. J. T., Meers, M. B., & Pendharkar, A. (2006). Biomechanics of the rostrum in crocodilians: A comparative analysis using finite-element modeling. *The Anatomical Record. Part A, Discoveries in Molecular, Cellular, and Evolutionary Biology*, *288*, 827–849.

Menegaz, R. A., Sublett, S. V., Figueroa, S. D., Hoffman, T. J., Ravosa, M. J., & Aldridge, K. (2010). Evidence for the influence of diet on cranial form and robusticity. *Anatomical Record*, *293*, 630–641.

Metzger, K. A., Daniel, W. J. T., & Ross, C. F. (2005). Comparison of beam theory and finite-element analysis with in vivo bone strain data from the alligator cranium. *Anatomical Record*, *283*, 331–348.

Montefeltro, F. C., Lautenschlager, S., Godoy, P. L., Ferreira, G. S., & Butler, R. J. (2020). A unique predator in a unique ecosystem: Modelling the apex predator within a Late Cretaceous crocodyliform-dominated fauna from Brazil. *Journal of Anatomy*, *237*, 323–333.

Morris, Z. S., Vliet, K. A., Abzhanov, A., & Pierce, S. E. (2019). Heterochronic shifts and conserved embryonic shape underlie crocodylian craniofacial disparity and convergence. *Proceedings of the Royal Society B: Biological Sciences*, *286*, 20182389.

Narváez, I., Brochu, C. A., Escaso, F., Pérez-Garcéa, A., & Ortega, F. (2015). New crocodyliforms from southwestern Europe and definition of a diverse clade of European late cretaceous basal eusuchians. *PLoS One*, *10*, 1–34.

Nesbitt, S. J. (2011). The early evolution of archosaurs: Relationships and the origin of major clades. *Bulletin of the American Museum of Natural History*, *352*, 1–292.

Nieto, M. N., Degrange, F. J., Sellers, K. C., Pol, D., & Holliday, C. M. (2021). Biomechanical performance of the cranio-mandibular complex of the small notosuchian *Araripesuchus gomesii* (Notosuchia, Uruguaysuchidae). *The Anatomical Record*, *305*(10), 2695–2707.

Norell, M. A., & Clark, J. M. (1990). A reanalysis of *Bernissartia fagesii*, with comments on its phylogenetic position and its bearing on the origin and diagnosis of the Eusuchia. *Bulletin de l'Institut Royal des Sciences Naturelles de Belgique*, *60*, 115–128.

O'Brien, H. D., Lynch, L. M., Vliet, K. A., Brueggen, J., Erickson, G. M., & Gignac, P. M. (2019). Crocodylian head width allometry and phylogenetic prediction of body size in extinct suchians. *Integrative Organismal Biology*, *1*, obz006.

Ősi, A. (2008). Cranial osteology of Iharkutosuchus makadii, a Late Cretaceous basal eusuchian crocodyliform from Hungary. *Neues Jahrbuch fur Geologie und Palaontologie - Abhandlungen*, *248*, 279–299.

Ősi, A. (2014). The evolution of jaw mechanism and dental function in heterodont crocodyliforms. *Historical Biology*, *26*, 279–414.

Ősi, A., Clark, J. M., & Weishampel, D. B. (2007). First report on a new basal eusuchian crocodyliform with multicusped teeth from the Upper Cretaceous (Santonian) of Hungary. *Neues Jahrbuch fur Geologie und Palaontologie - Abhandlungen*, *243*, 169–177.

Parker, W. G., Nesbitt, S. J., Irmis, R. B., Martz, J. W., Marsh, A. D., Brown, M. A., Stocker, M. R., & Werning, S. (2021). Osteology and relationships of *Revueltosaurus callenderi* (Archosauria: Suchia) from the upper Triassic (Norian) Chinle formation of petrified Forest National Park, Arizona, United States. *The Anatomical Record*, *305*(10), 2353–2414.

Perry, J. M. G., Hartstone-Rose, A., & Logan, R. L. (2011). The jaw adductor resultant and estimated bite force in primates. *Anatomy Research International*, *2011*, 929848.

Pierce, S. E., Angielczyk, K. D., & Rayfield, E. J. (2009). Shape and mechanics in thalattosuchian (Crocodylomorpha) skulls: Implications for feeding behaviour and niche partitioning. *Journal of Anatomy*, *215*, 555–576.

Pierce, S. E., & Benton, M. J. (2006). *Pelagosaurus typus* Bronn, 1841 (Mesoeucrocodylia: Thalattosuchia) from the upper Lias (Toarcian, lower Jurassic) of Somerset, England. *Journal of Vertebrate Paleontology*, *26*, 621–635.

Pol, D., & Leardi, J. M. (2015). *Diversity patterns of Notosuchia (Crocodyliformes, Mesoeucrocodylia) during the Cretaceous of Gondwana*. Publicación Electrónica la Asociación Paleontológica Argentina.

Pol, D., Nascimento, P. M., Carvalho, A. B., Riccomini, C., Pires-Domingues, R. A., & Zaher, H. (2014). A new notosuchian from the late cretaceous of Brazil and the phylogeny of advanced notosuchians. *PLoS One*, *9*, e93105.

Pol, D., Rauhut, O. W. M., Lecuona, A., Leardi, J. M., Xu, X., & Clark, J. M. (2013). A new fossil from the Jurassic of Patagonia reveals the early basicranial evolution and the origins of Crocodyliformes. *Biological Reviews of the Cambridge Philosophical Society*, *88*, 862–872.

Porro, L. B., Holliday, C. M., Anapol, F., Ontiveros, L. C., Ontiveros, L. T., & Ross, C. F. (2011). Free body analysis, beam mechanics, and finite element modeling of the mandible of *Alligator mississippiensis*. *Journal of Morphology*, *272*, 910–937.

Porro, L. B., Metzger, K. A., Iriarte-Díaz, J., & Ross, C. F. (2013). In vivo bone strain and finite element modeling of the mandible of *Alligator mississippiensis*. *Journal of Anatomy*, *223*, 195–227.

Ruebenstahl, A. A. (2019). *Junggarsuchus sloani, an early late Jurassic Crocodylomorph with Crocodyliform affinities* (MS Thesis). George Washington University.

Sacks, R. D., & Roy, R. R. (1982). Architecture of the hind limb muscles of cats: Functional significance. *Journal of Morphology*, *173*, 185–195.

Salisbury, S. W., Molnar, R. E., Frey, E., & Willis, P. M. A. (2006). The origin of modern crocodyliforms: New evidence from the cretaceous of Australia. *Proceedings of the Biological Sciences*, *273*, 2439–2448.

Santana, S. E., Dumont, E. R., & Davis, J. L. (2010). Mechanics of bite force production and its relationship to diet in bats. *Functional Ecology*, *24*, 776–784.

Schumacher, G.-H. (1973). The head muscles and hyolaryngeal skeleton of turtles and crocodilians. In C. Gans (Ed.), *Biology of the Reptilia* (Vol. 4, pp. 101–199). Academic Press.

Sellers, K. C., Middleton, K. M., Davis, J. L., & Holliday, C. M. (2017). Ontogeny of bite force in a validated biomechanical model of the American alligator. *The Journal of Experimental Biology*, *220*, 2036–2046.

Sereno, P. C., & Larsson, H. C. E. (2009). Cretaceous crocodyliforms from the Sahara. *Zookeys*, *28*, 1–143.

Stubbs, T. L., Pierce, S. E., Elsler, A., Anderson, P. S. L., Rayfield, E. J., & Benton, M. J. (2021). Ecological opportunity and the rise and fall of crocodylomorph evolutionary innovation. *Proceedings of the Royal Society B*, *288*, 20210069.

Tarsitano, S. F. (1985). Cranial metamorphosis and the origin of the Eusuchia. *Neues Jahrbuch für Geologie und Paläontologie*, *170*, 27–44.

Team, R. C. (2021). R: A language and environment for statistical computing. Vienna, Austria: R Foundation for Statistical Computing. https://www.R-project.org/.

Tsai, H. P., & Holliday, C. M. (2011). Ontogeny of the alligator cartilago transiliens and its significance for sauropsid jaw muscle evolution. *PLoS One*, *6*, e24935.

Tseng, Z. J., & Stynder, D. (2011). Mosaic functionality in a transitional ecomorphology: Skull biomechanics in stem Hyaeninae compared to modern South African carnivorans. *Biological Journal of the Linnean Society*, *102*, 540–559.

Tseng, Z. J., & Wang, X. (2010). Cranial functional morphology of fossil dogs and adaptation for durophagy in *Borophagus* and *Epicyon* (Carnivora, Mammalia). *Journal of Morphology*, *271*, 1386–1398.

Turner, A. H. (2015). A review of *Shamosuchus* and *Paralligator* (Crocodyliformes,Nneosuchia) from the Cretaceous of Asia. *PLoS One*, *10*, 1–39.

Turner, A. H., & Buckley, G. A. (2008). *Mahajangasuchus insignis* (Crocodyliformes: Mesoeucrocodylia) cranial anatomy and new data on the origin of the eusuchian-style palate. *Journal of Vertebrate Paleontology*, *28*, 382–408.

Turner, A. H., & Sertich, J. J. W. (2010). Phylogenetic history of *Simosuchus clarki* (Crocodyliformes: Notosuchia) from the late cretaceous of Madagascar. *Journal of Vertebrate Paleontology*, *30*, 177–236.

Walmsley, C. W., Smits, P. D., Quayle, M. R., McCurry, M. R., Richards, H. S., Oldfield, C. C., Wroe, S., Clausen, P. D., & McHenry, C. R. (2013). Why the long face? The mechanics of mandibular symphysis proportions in crocodiles. *PLoS One*, *8*, e53873.

Weijs, W. A., Brugman, P., & Klok, E. M. (1987). The growth of the skull and jaw muscles and its functional consequences in the New Zealand rabbit (*Oryctolagus cuniculus*). *Journal of Morphology*, *194*, 143–161.

Wilberg, E. W. (2017). Investigating patterns of crocodyliform cranial disparity through the mesozoic and cenozoic. *Zoological Journal of the Linnean Society*, *181*, 189–208.

Wilberg, E. W., Turner, A. H., & Brochu, C. A. (2019). Evolutionary structure and timing of major habitat shifts in Crocodylomorpha. *Scientific Reports*, *9*, 514.

Wilken, A. T., Middleton, K. M., Sellers, K. C., Cost, I. N., & Holliday, C. M. (2019). The roles of joint tissues and jaw muscles in palatal biomechanics of the Savannah monitor (*Varanus exanthematicus*) and their significance for cranial kinesis. *The Journal of Experimental Biology*, *222*, jeb.201459.

Wilken, A. T., Sellers, K. C., Cost, I. N., Rozin, R. E., Middleton, K. M., & Holliday, C. M. (2020). Connecting the chondrocranium: Biomechanics of the suspensorium in reptiles. *Vertebrate Zoology*, *70*, 275–290.

Witmer, L. M. (1995). The extant phylogenetic bracket and the importance of reconstructing soft tissue in fossils. *Functional Morphology in Vertebrate Paleontology*, *1*, 19–33.

Witmer, L. M. (1997). The evolution of the Antorbital cavity of archosaurs: A study in soft-tissue reconstruction in the fossil record with an analysis of the function of Pneumaticity. *Journal of Vertebrate Paleontology*, *17*, 1–76.

Wu, X. C., Brinkman, D. B., & Lu, J. C. (1994). A new species of *Shantungosuchus* from the lower cretaceous of Inner Mongolia (China), with comments on *S. chuhsienensis* Young, 1961 and the phylogenetic position of the genus. *Journal of Vertebrate Paleontology*, *14*, 210–229.

Wu, X.-C., Sues, H.-D., & Dong, Z.-M. (1997). *Sichuanosuchus shuhanensis*, a new ?Early Cretaceous Protosuchian (Archosauria: Crodocylifoems) from Sichuan (China), and the monophyly of Protosuchia. *Journal of Vertebrate Paleontology*, *17*, 89–103.

SUPPORTING INFORMATION

Additional supporting information may be found in the online version of the article at the publisher's website.

How to cite this article: Sellers, K. C., Nieto, M. N., Degrange, F. J., Pol, D., Clark, J. M., Middleton, K. M., & Holliday, C. M. (2022). The effects of skull flattening on suchian jaw muscle evolution. *The Anatomical Record*, *305*(10), 2791–2822. https://doi.org/10.1002/ar.24912

APPENDIX A

TABLE A1 Table of links to Sketchfab models of skulls with muscle vectors. Extinct taxa are indicated with dagger symbol (†)

Taxon	Sketchfab Link
Alligator mississippiensis	https://sketchfab.com/3d-models/alligator-mississippiensis-muvc-al-008-16194d93499943c2ae3822d61d7cf224
Caiman crocodilus	https://sketchfab.com/3d-models/caiman-crocodilus-fmnh-73711-8bd5c465e7314e01ba5301d4f52b585e
Paleosuchus palpebrosus	https://sketchfab.com/3d-models/paleosuchus-palpebrosus-fmnh-22817-4f0011a16cfc45e4825311e6aafcc2b3
Crocodylus moreletii	https://sketchfab.com/3d-models/crocodylus-moreletii-tmm-m-4980-3d87992f50434bfb8d762bd2a3d41994
Osteolaemus tetraspis	https://sketchfab.com/3d-models/osteolaemus-tetraspis-fmnh-98936-05a5cf629180442a9b3544a05ca1d89d
Tomistoma schlegelii	https://sketchfab.com/3d-models/tomistoma-schlegelii-tmm-m-6342-8f55af4d68c44576a7b3c42853860c0e
†*Araripesuchus gomesii*	https://sketchfab.com/3d-models/araripesuchus-gomesii-amnh-24450-d6e8b073dda0473fa01dbb3a7cf7df05
†*"Gomphosuchus" sp.*	https://sketchfab.com/3d-models/gomphosuchus-sp-ucmp-97638-00f2938264ff4d8f9cf5429dbb270f95
†*Junggarsuchus sloani*	https://sketchfab.com/3d-models/junggarsuchus-sloani-ivpp-v14010-bd9b74731cf44940bab6c95d36877793
†*Prestosuchus chiniquensis*	https://sketchfab.com/3d-models/prestosuchus-chiniquensis-ufrgs-pv0629t-e8d8f971abc44b699790d56cae026589
†*Revueltosaurus callenderi*	https://sketchfab.com/3d-models/revueltosaurus-callenderi-pefo-34561-dfbd608848814e518a62713d266a916f

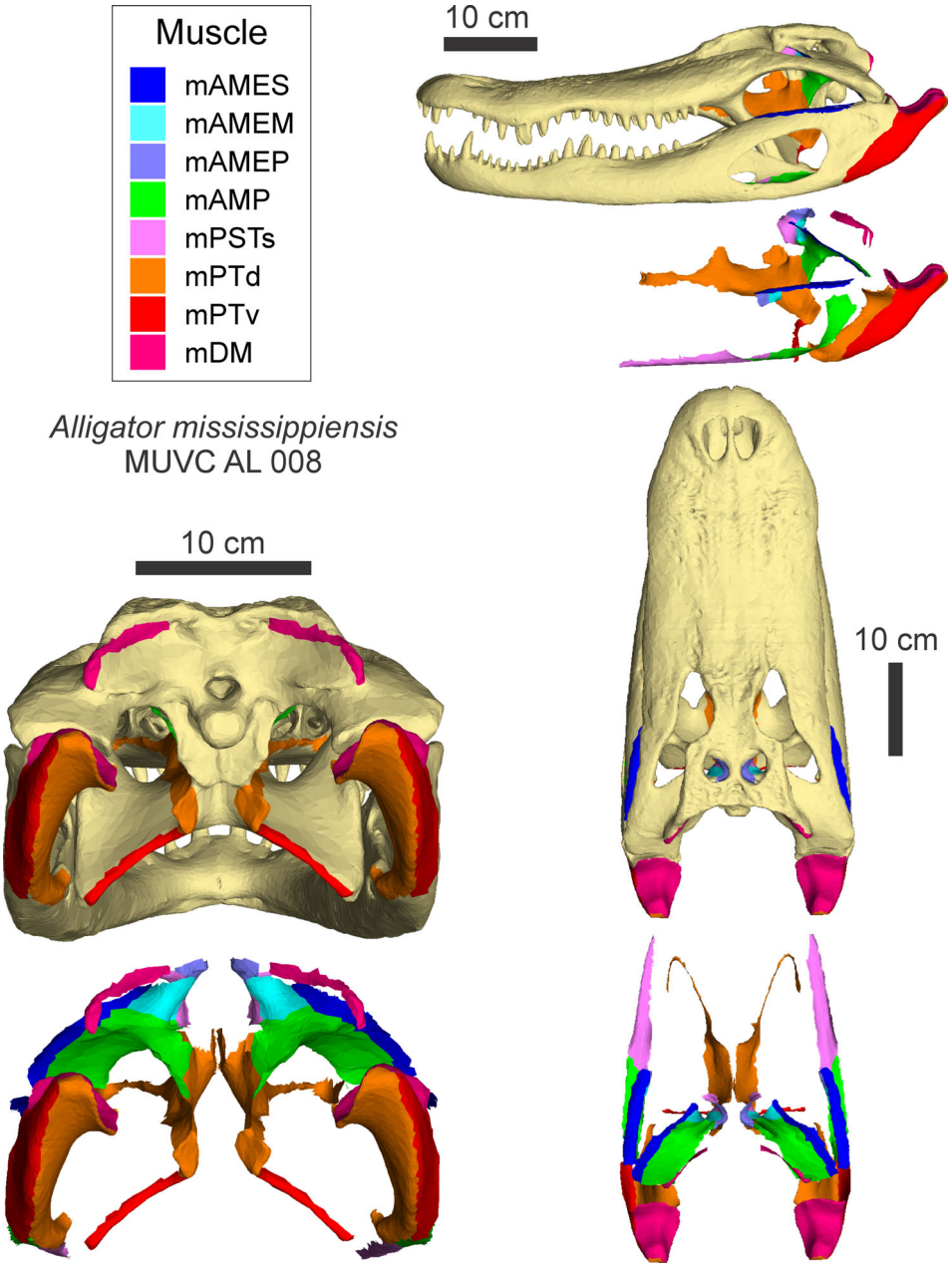

FIGURE A1 Muscle attachments in *Alligator mississippiensis*. Top-left, muscle homology color scheme. Top-right, left lateral view. Bottom-left, caudal view. Bottom-right, dorsal view

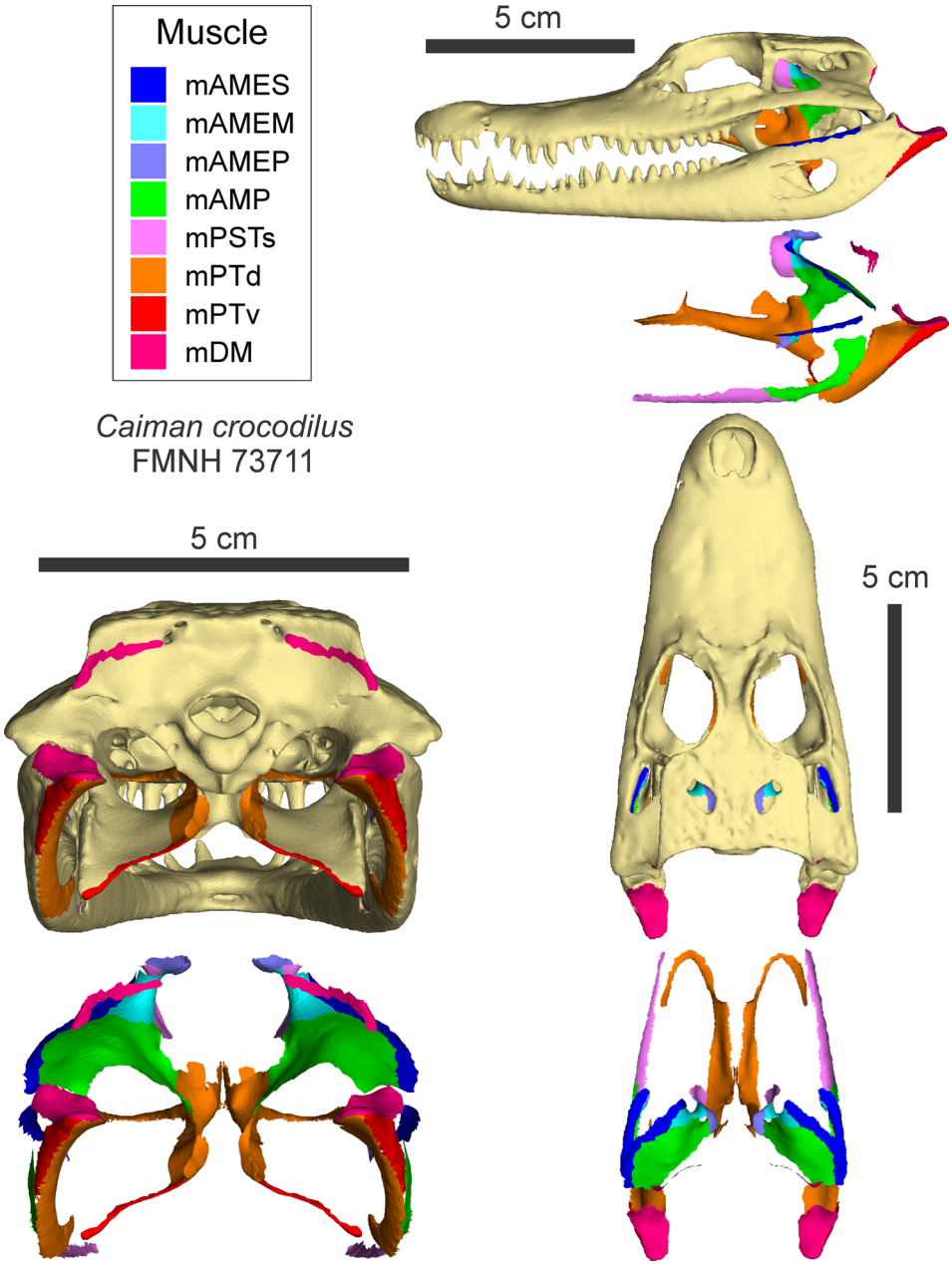

FIGURE A2 Muscle attachments in *Caiman crocodilus*. Top-left, muscle homology color scheme. Top-right, left lateral view. Bottom-left, caudal view. Bottom-right, dorsal view

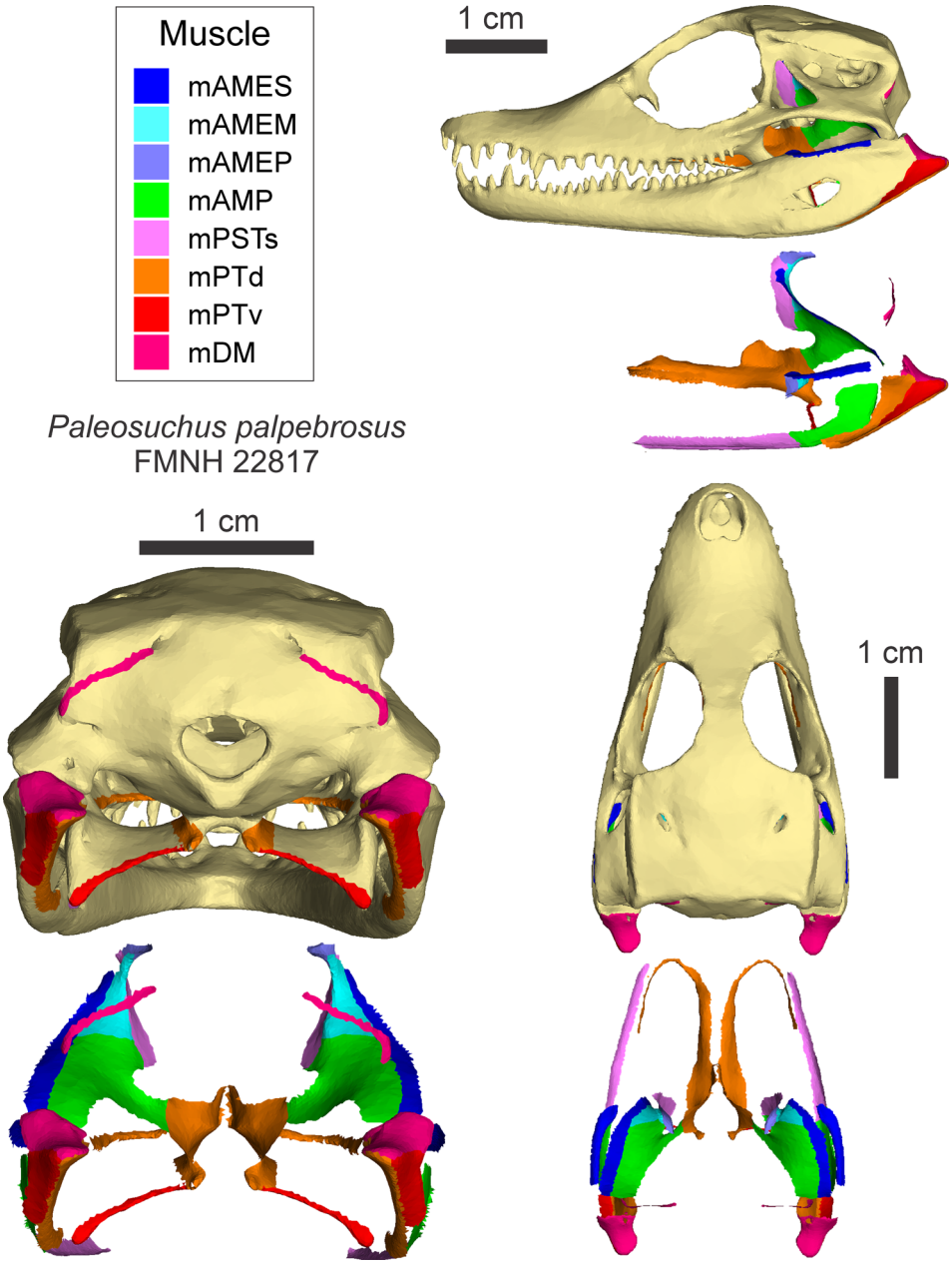

FIGURE A3 Muscle attachments in *Paleosuchus palpebrosus*. Top-left, muscle homology color scheme. Top-right, left lateral view. Bottom-left, caudal view. Bottom-right, dorsal view

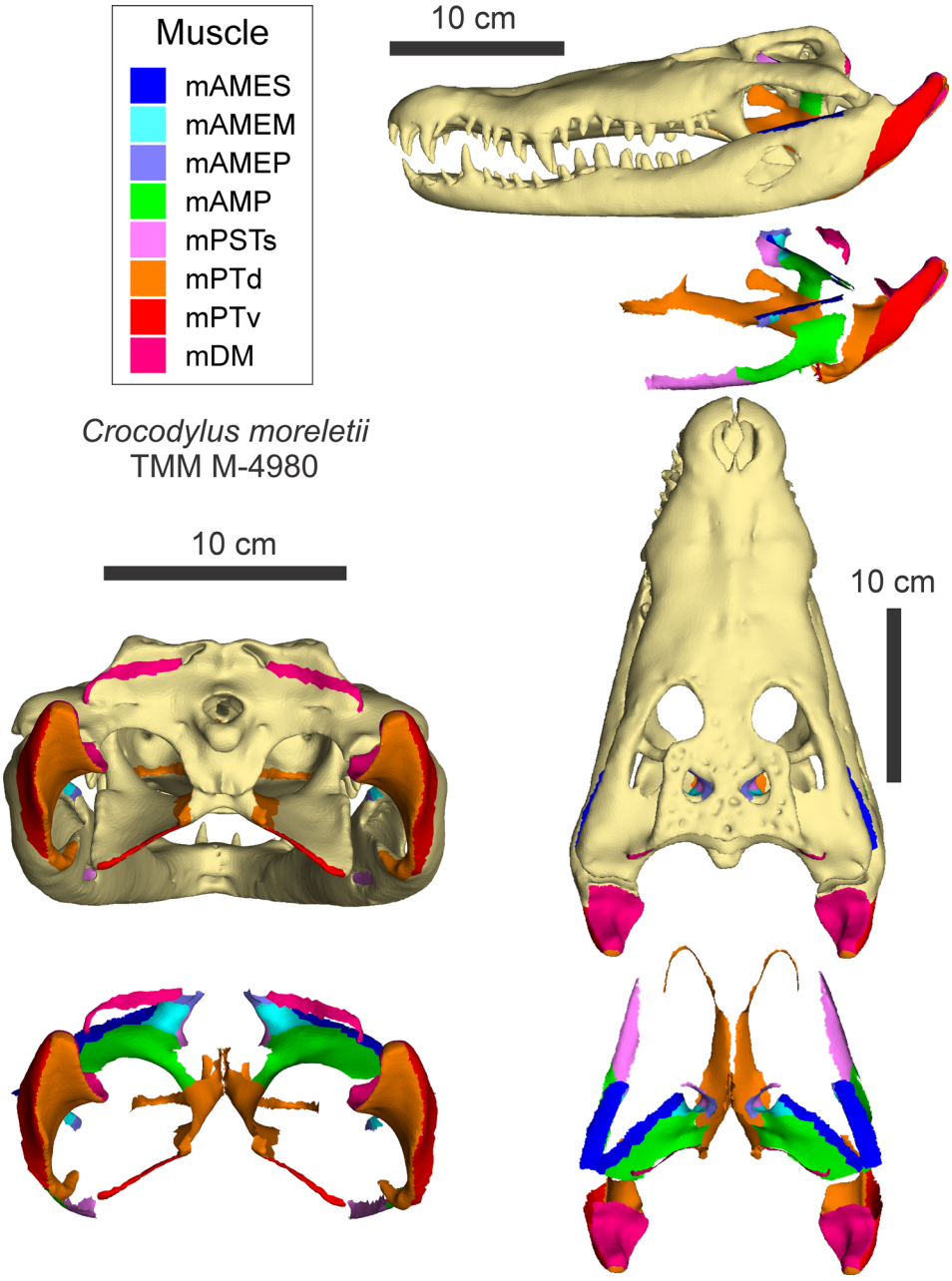

FIGURE A4 Muscle attachments in *Crocodylus moreletii*. Top-left, muscle homology color scheme. Top-right, left lateral view. Bottom-left, caudal view. Bottom-right, dorsal view

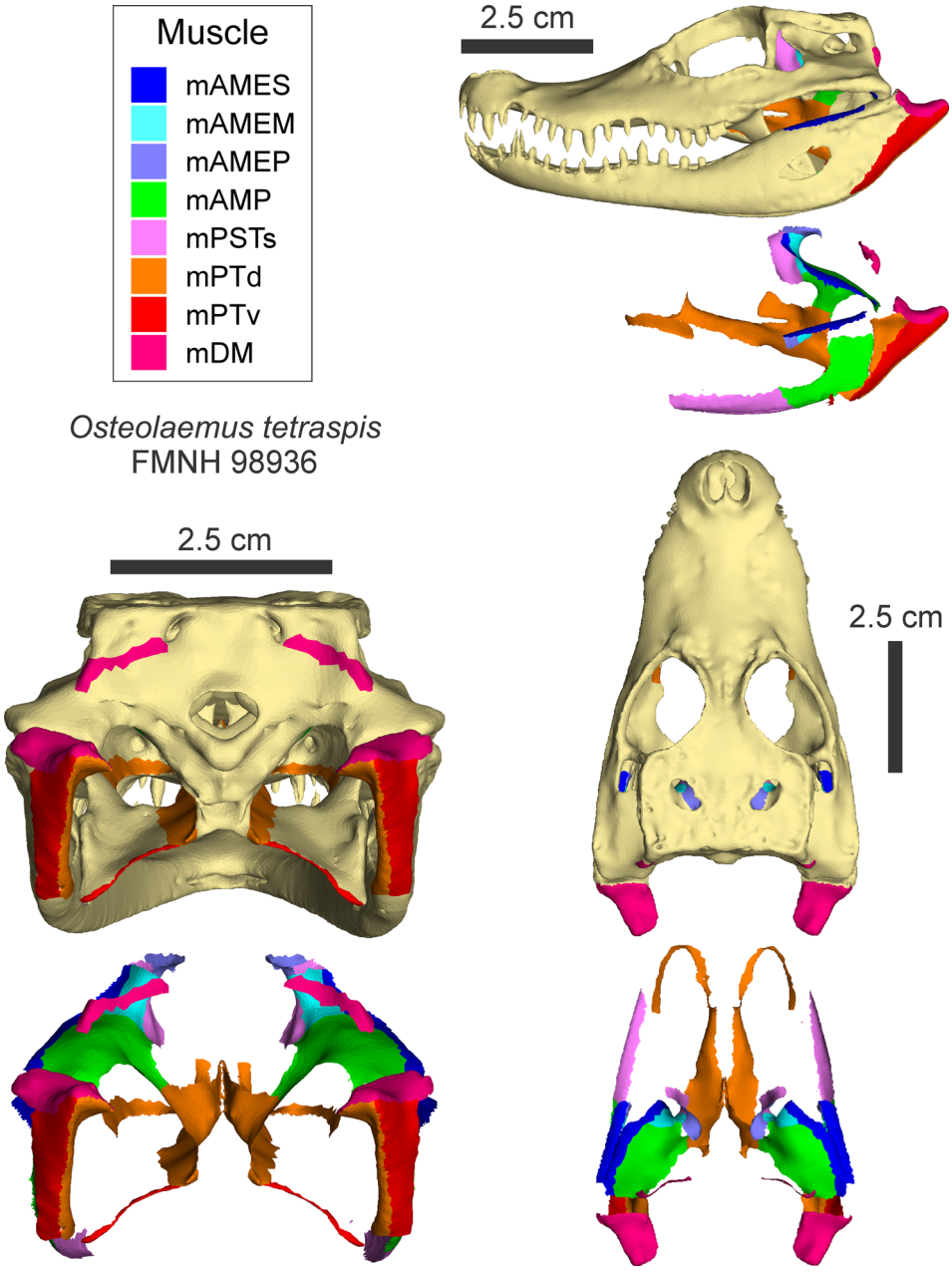

FIGURE A5 Muscle attachments in *Osteolaemus tetraspis*. Top-left, muscle homology color scheme. Top-right, left lateral view. Bottom-left, caudal view. Bottom-right, dorsal view

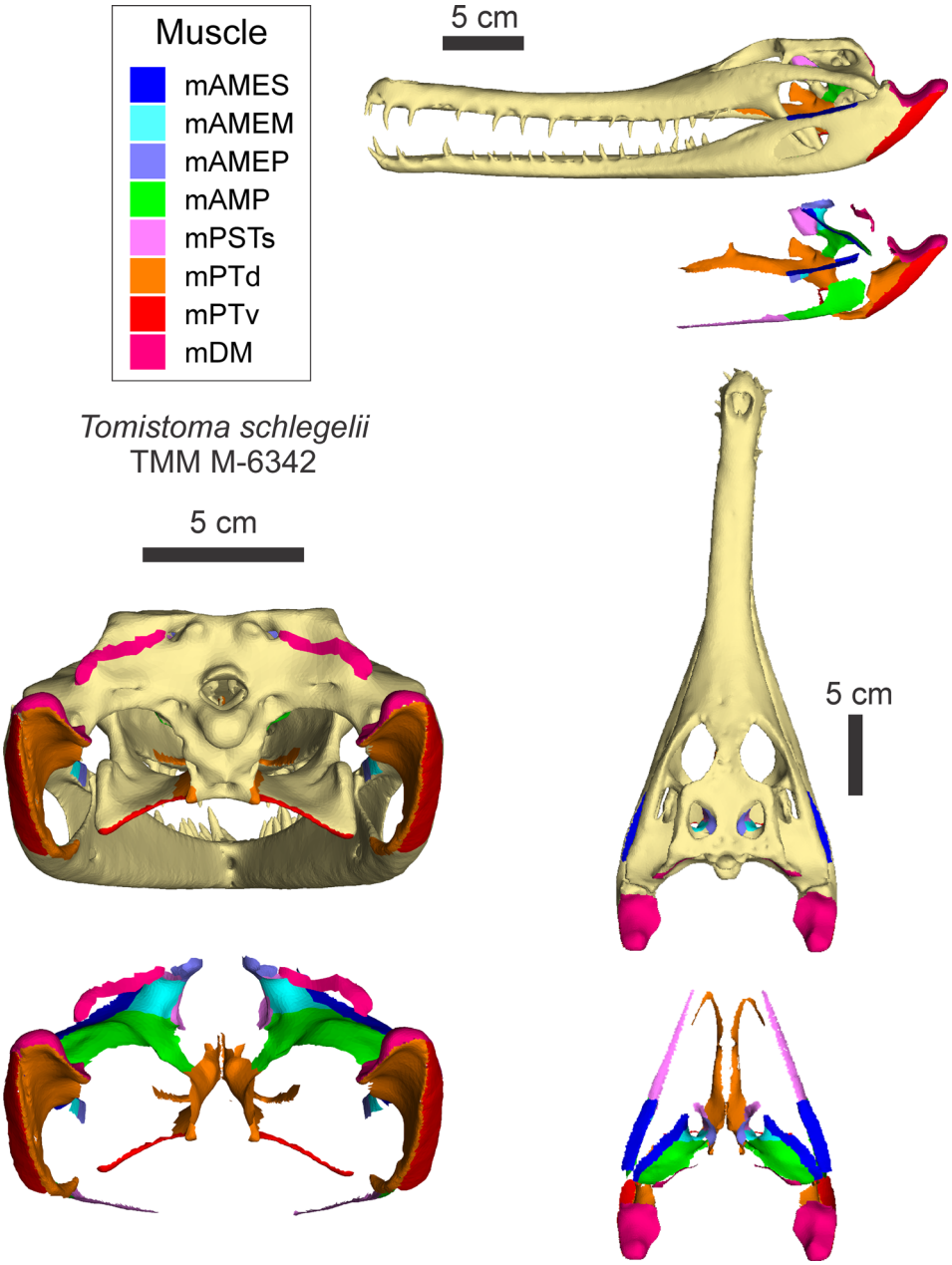

FIGURE A6 Muscle attachments in *Tomistoma schlegelii*. Top-left, muscle homology color scheme. Top-right, left lateral view. Bottom-left, caudal view. Bottom-right, dorsal view

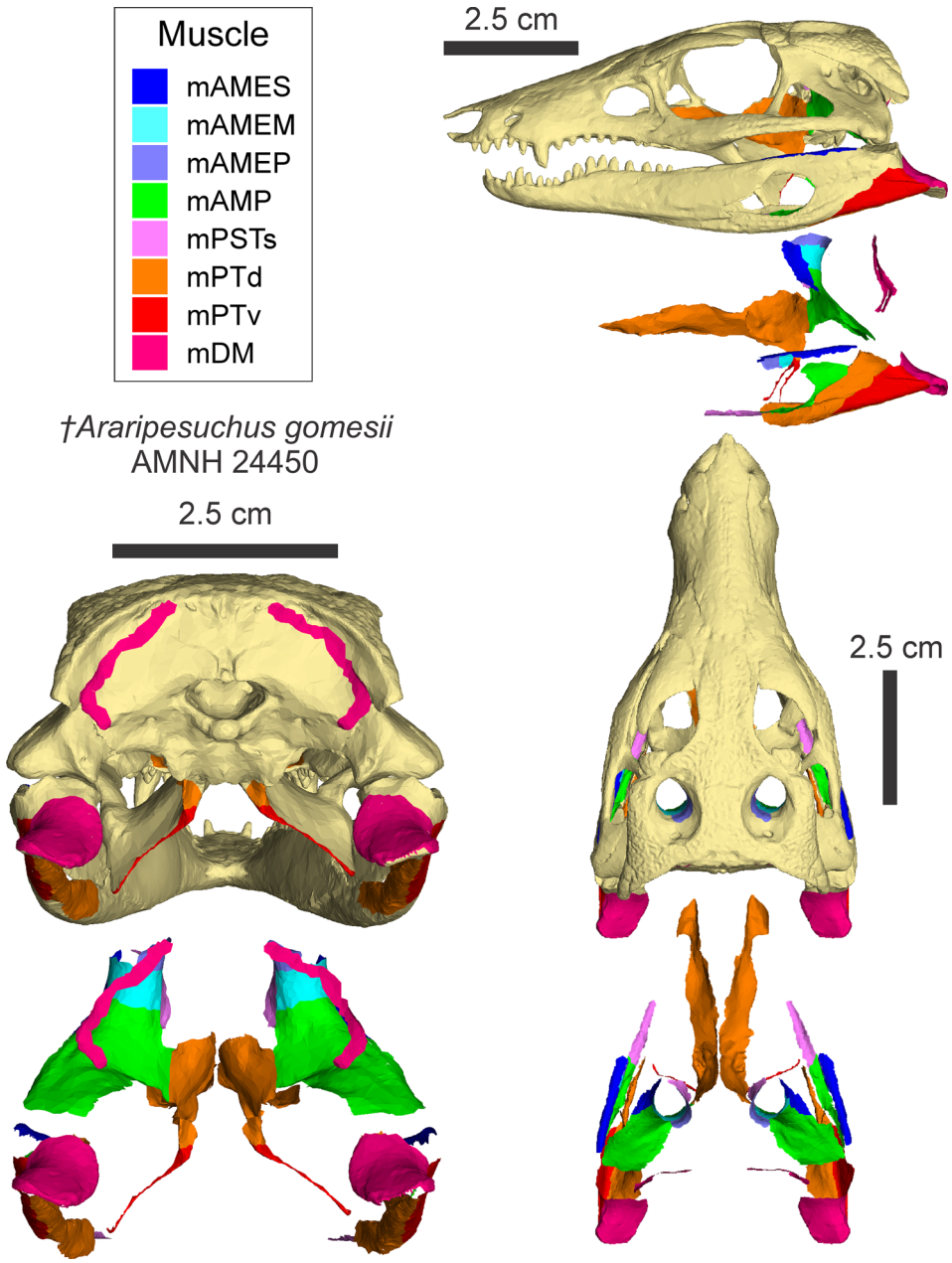

FIGURE A7 Muscle attachments in †*Araripesuchus gomesii*. Top-left, muscle homology color scheme. Top-right, left lateral view. Bottom-left, caudal view. Bottom-right, dorsal view

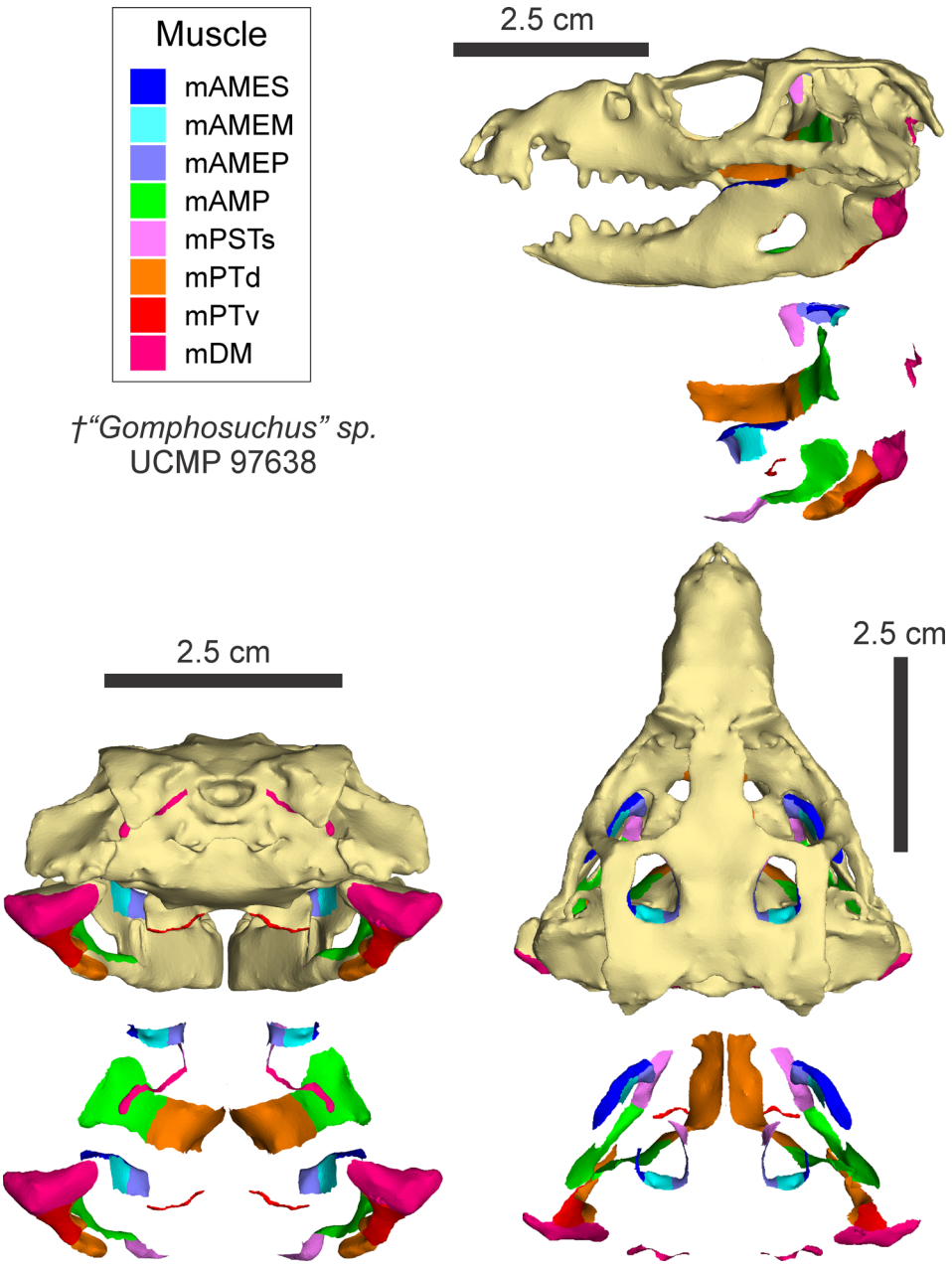

FIGURE A8 Muscle attachments in † "*Gomphosuchus* sp." Top-left, muscle homology color scheme. Top-right, left lateral view. Bottom-left, caudal view. Bottom-right, dorsal view

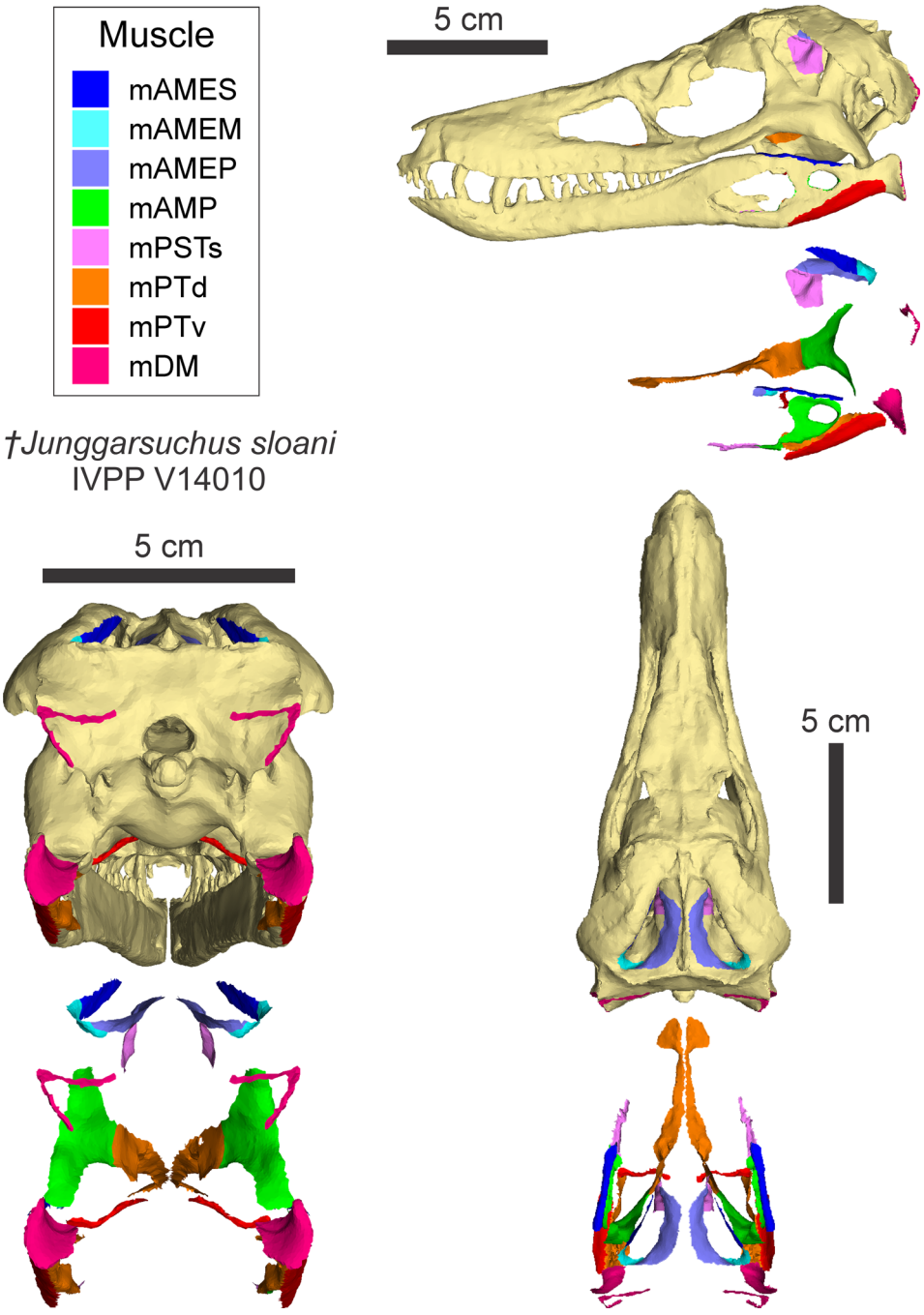

FIGURE A9 Muscle attachments in †*Junggarsuchus sloani*. Top-left, muscle homology color scheme. Top-right, left lateral view. Bottom-left, caudal view. Bottom-right, dorsal view

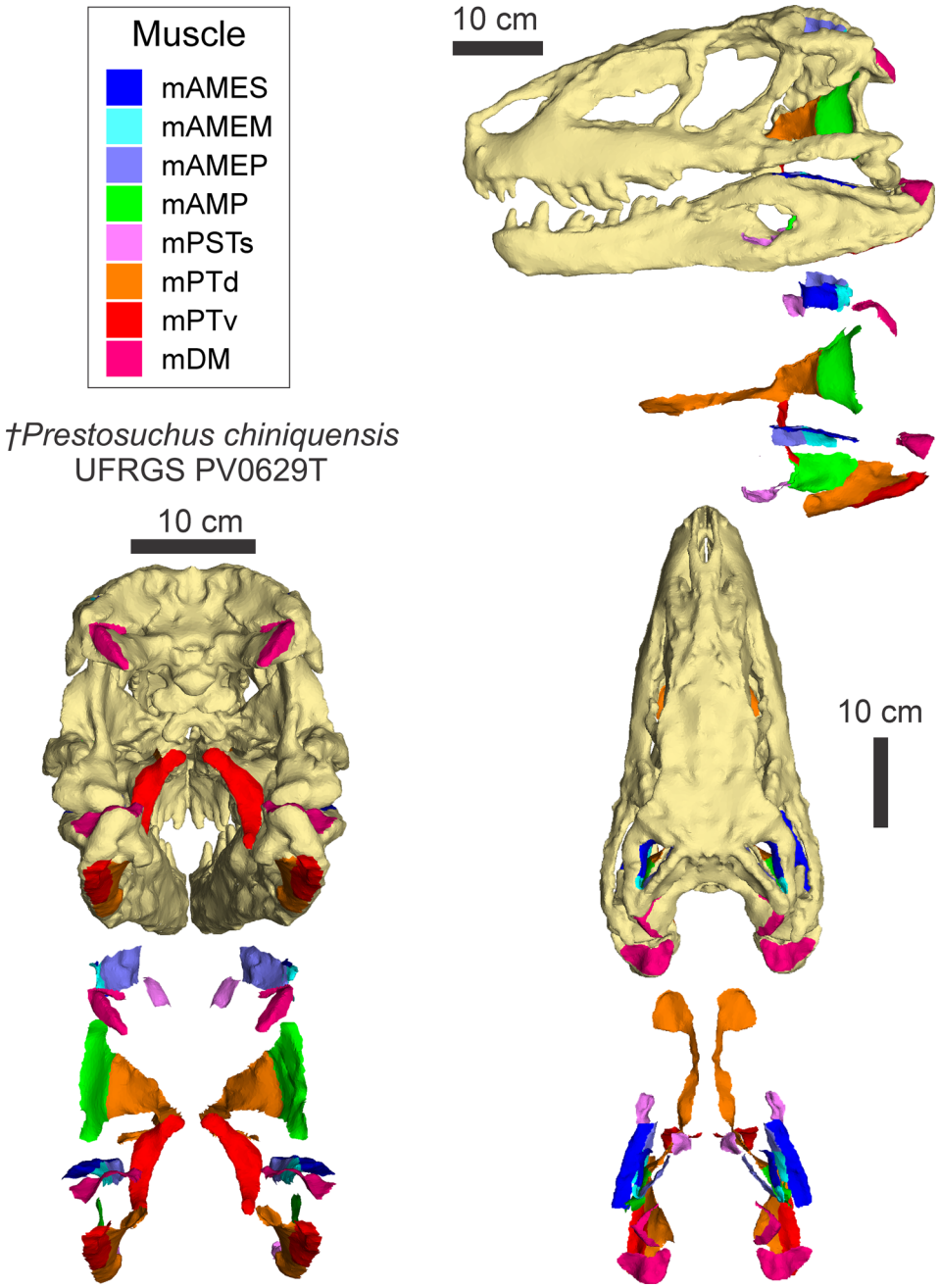

FIGURE A10 Muscle attachments in †*Prestosuchus chiniquensis*. Top-left, muscle homology color scheme. Top-right, left lateral view. Bottom-left, caudal view. Bottom-right, dorsal view

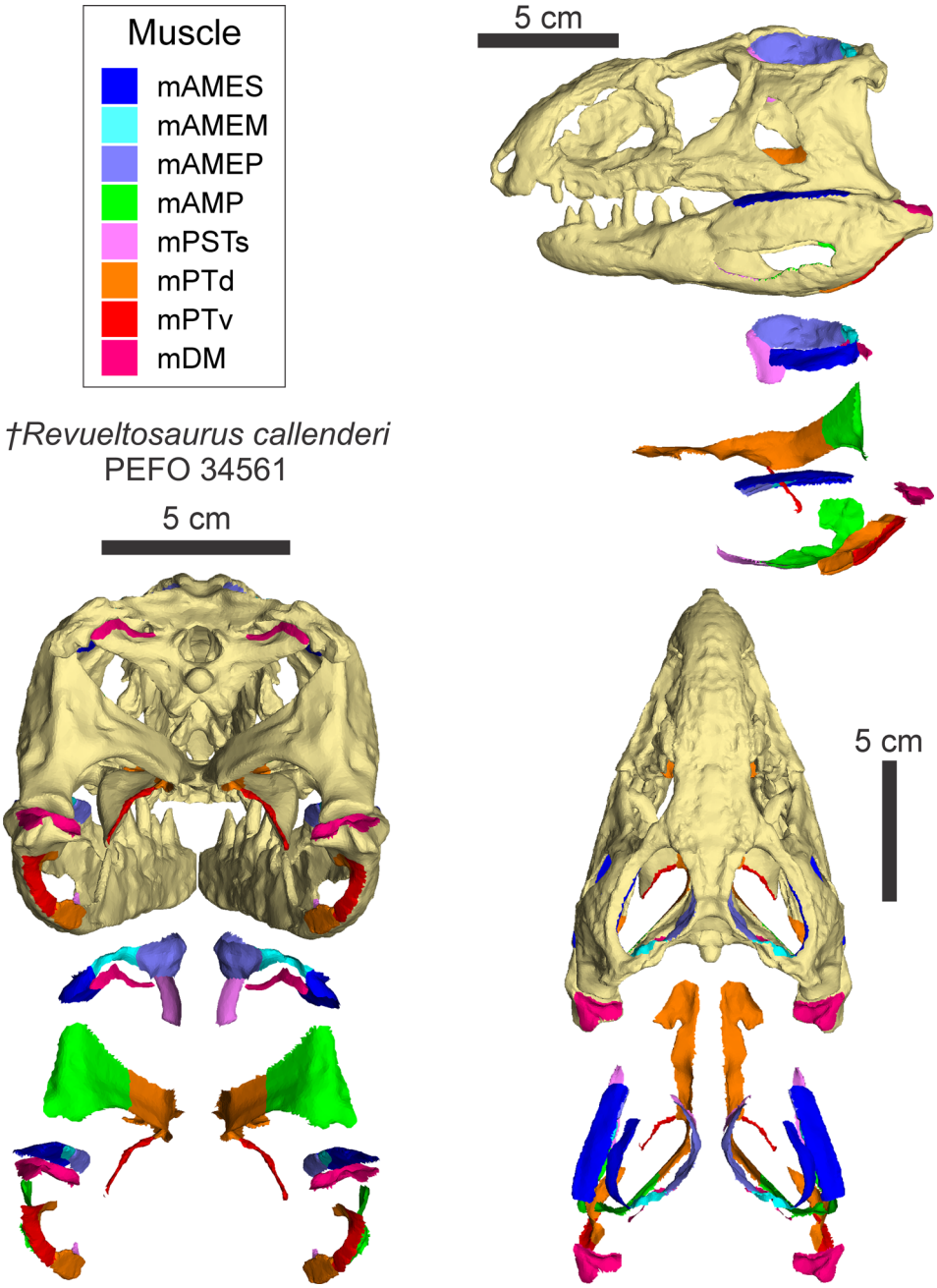

FIGURE A11 Muscle attachments in †*Revueltosaurus callenderi*. Top-left, muscle homology color scheme. Top-right, left lateral view. Bottom-left, caudal view. Bottom-right, dorsal view